

# Why is the city's responsibility for its air pollution often underestimated? A focus on PM<sub>2.5</sub>

Philippe Thunis<sup>1</sup>, Alain Clappier<sup>2</sup>, Alexander de Meij<sup>3</sup>, Enrico Pisoni<sup>1</sup>, Bertrand Bessagnet<sup>1</sup>, Leonor Tarrason<sup>4</sup>.

<sup>1</sup> European Commission, Joint Research Centre, Ispra, Italy

<sup>2</sup> Université de Strasbourg, Laboratoire Image Ville Environnement, Strasbourg, France

<sup>3</sup> MetClim, Varese, Italy

<sup>4</sup> NILU, Norway

*Correspondence to:* Philippe Thunis (philippe.thunis@ec.europa.eu)

## Abstract

While the burden caused by air pollution in urban areas is well documented, the origin of this pollution and therefore the responsibility of the urban areas in generating this pollution is still a subject of scientific discussion. Source Apportionment represents a useful technique to quantify the city responsibility but the approaches and applications are not harmonized, therefore not comparable, resulting in confusing and sometimes contradicting interpretations. In this work, we analyze how different source apportionment approaches apply to the urban scale and how their building elements and parameters are defined and set. We discuss in particular the options available in terms of indicator, receptor, source and methodology. We show that different choices for these options lead to very large differences in terms of outcome. For the 150 EU large cities selected in our study, different choices made for the indicator, the receptor and the source each lead to an average factor 2 difference in terms of city contribution. We also show that temporal and spatial averaging processes applied to the air quality indicator, especially when diverging source apportionments are aggregated into a single number lead to favor strategies that target background sources while occulting actions that would be efficient at the city center. We stress that methodological choices and assumptions most often lead to a systematic and important underestimation of the city responsibility, with important implications. Indeed, if cities are seen as a minor actor, plans will target in priority the background at the expense of potentially effective local actions.

**Keywords:** air pollution, source apportionment, particulate matter

## 1. Introduction

About 55% of the world's population lives in urban areas nowadays, and this number is expected to increase to 68% by 2050, according to the United Nations (UN 2018). Large population growth is also projected by 2030 in most of the major European cities (Alberti et al., 2019) with predicted population growth varying in range from Berlin (15%), Paris (19%), Milan/Rome

41 (21%), Prague (37%), London (39%), to Brussels (52%) (see  
42 <https://urban.jrc.ec.europa.eu/thefutureofcities/urbanisation#the-chapter>). As a result of this  
43 population trend, urban emissions and their associated pollution levels are expected to increase  
44 as well.

45  
46 According to a recent estimate (EEA, 2020), about 74 % of the EU-28 urban population are  
47 exposed to pollution of fine particulate matter (PM<sub>2.5</sub>) in concentrations above the WHO Air  
48 Quality Guidelines value, this number raises to 99% for ozone (O<sub>3</sub>) and is about 4% for nitrogen  
49 dioxide (NO<sub>2</sub>). Air pollution is a heavy burden on human health with more than 380,000  
50 premature deaths in EU-28 reported in 2017 according to the same EEA estimates. For a wide  
51 range of European cities, Khomenko et al. (2021) showed that the health burden due to air  
52 pollution varies greatly by city, with annual premature mortality reaching up to 15% for PM<sub>2.5</sub>  
53 and 7% for NO<sub>2</sub>. The highest mortality burden for PM<sub>2.5</sub> occurs in northern Italy, southern  
54 Poland and eastern Czech Republic. De Bruyn and de Vries (2020) showed that for all 432 cities  
55 in their sample (total population: 130 million inhabitants), the social costs (e.g. hospital  
56 admissions, premature mortality) but also due to air pollution exceeded € 166 billion in 2018 for  
57 Europe (EU27 plus the UK, Norway and Switzerland). City size was shown to be a key factor  
58 contributing to the total social costs: all cities with a population over 1 million features in the  
59 Top 25 cities with the highest social costs due to air pollution.

60  
61 Given the health and economic burden caused by air pollution in urban areas, it is important to  
62 identify the origin of this pollution in order to reduce and control its impact. Identifying the  
63 sources of urban pollution and then assigning responsibilities enables a process to implement  
64 measures and control air pollution. Assessing the responsibility or share of cities for their  
65 pollution has important implications. For being effective, pollution reduction plans must be  
66 designed and applied to target the most polluting sectors at the relevant spatial (national, regional  
67 and/or local) and with the appropriate temporal scales. In this context, quantifying the share or  
68 the city pollutions caused by their own emissions becomes a crucial element to determine  
69 whether actions need to be applied locally or at the regional, national country or continental  
70 scales. This has important governance consequences for the effective control of air pollution.

71  
72 For pollutants like NO<sub>2</sub>, that mostly originate from traffic sources and have a relatively short  
73 lifetime in the atmosphere, there is a general agreement on the fact that cities are the main  
74 contributor to this pollutant concentration levels and that acting locally on traffic emissions is the  
75 most efficient way of improving NO<sub>2</sub> concentration levels in a particular city (Tobias et al.,  
76 2020). There is available European-wide information such as in Degraeuwe et al. (2019)  
77 providing overviews of the potential impact of traffic emission reductions per vehicle type in  
78 different European cities. There is also agreement regarding O<sub>3</sub> that this secondary pollutant is  
79 most effectively reduced by implementing reduction measures at larger spatial scales, involving  
80 actions driven at the regional and even continental scales (e.g. Luo et al. 2020). For other  
81 pollutants, like PM<sub>2.5</sub>, complex physical and chemical atmospheric processes with different time  
82 scales drive its formation, involving numerous precursors themselves emitted by several sources.  
83 The sources of PM<sub>2.5</sub> pollution range from local traffic, domestic fuel burning and industrial  
84 activities to regional sources such as agriculture in rural areas. Even though the latter emissions  
85 do not originate from cities, Thunis et al. (2018) showed that their impact on urban pollution  
86 could be important, reaching up to 30% in several European cities. Because of this complexity,

87 there is less consensus regarding the responsibility or share of a city to its pollution when  
88 addressing PM<sub>2.5</sub>. Because of this lack of consensus and the major burden of PM<sub>2.5</sub> on health, we  
89 focus our analysis on this pollutant.

90  
91 The usual approach to assess the city share to its pollution levels (in other words the city  
92 responsibility) is source apportionment (SA). However, many SA approaches exist. The most  
93 widely used SA methods are the “potential impact” (or brute force), the “increment” and  
94 “tagging” approaches. An overview description of these methods and an evaluation of their  
95 limitations and capabilities for use can be found in Thunis et al. (2019). Moreover, many ways to  
96 parameterize them exist as well, leading to a variety of results and interpretations. For the 18  
97 million inhabitant’s city of New Delhi, Amann et al. (2017) concluded that only 40% of the  
98 PM<sub>2.5</sub> pollution was originating from local city sources, based on potential impacts SA and  
99 expressed in terms of city averaged population exposure, averaged yearly. In the context of the  
100 Copernicus programme, CAMS (Copernicus Atmosphere Monitoring Service) performs SA  
101 calculations daily with two different approaches, namely tagging and potential impacts, for a  
102 series of European cities. Results show important differences on a day-by-day basis although  
103 these differences smooth out when considering longer term averages (Pommier et al. 2020).  
104 Based on the increment approach, Kiesewetter and Amann (2014) derived SA estimates for a  
105 series of European cities and aggregated these detailed results at country levels, leading to  
106 relatively low city responsibilities (e.g. about 25% for French, German or Italian cities). Based  
107 on a potential impact approach, Thunis et al. (2018) estimated city shares for 150 cities in  
108 Europe. They highlighted their large variability across Europe and stressed the importance of the  
109 definition of the city on the results, by testing the sensitivity to different city extensions. The  
110 choice of the SA method but also the way this method is configured, can lead to very different  
111 outcomes for the city share to its pollution, ranging from cities being a major contributor to their  
112 pollution to cities having a limited responsibility. This explains why the actual city responsibility  
113 on its pollution is yet discussed, and why some authors stress the importance of local actions  
114 (Thunis et al., 2018, Wu et al. 2011, Raifman et al., 2020) when others stress the need for  
115 regional, national or even continental actions (Huszar et al. 2016, ApSimon et al. 2021, Liu et al.,  
116 2013). This diversity of conclusions has serious consequences in terms of policy decisions.  
117 Blaming external (i.e. outside the city) pollution sources as main responsible for urban pollution  
118 is sometimes an easy argumentation for decision-makers to justify local inaction.

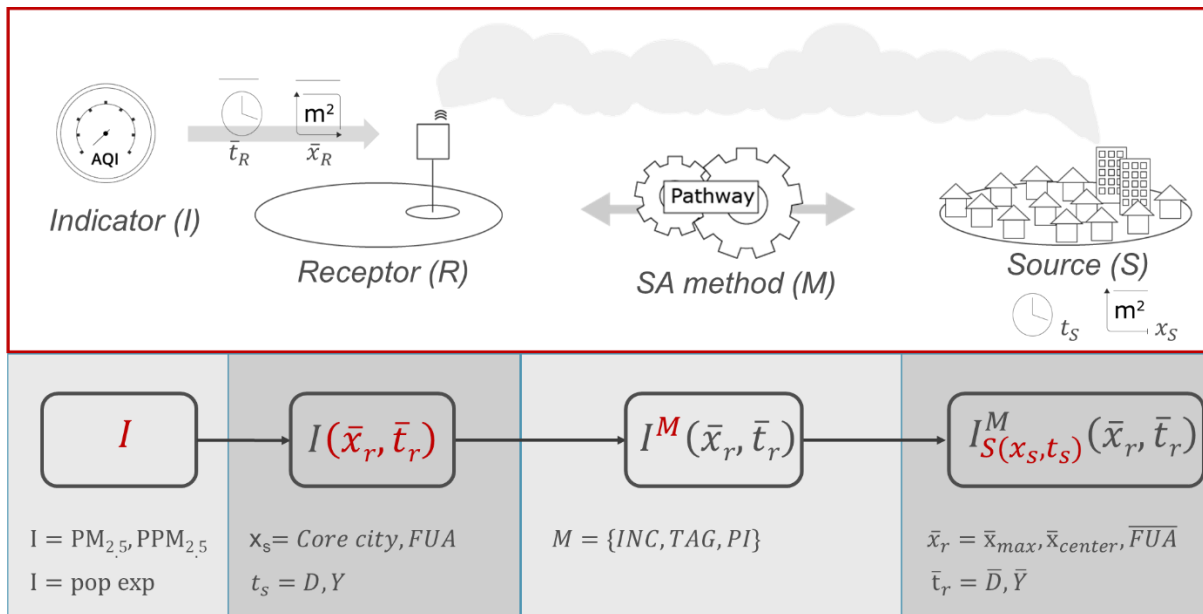
119  
120 This work aims at explaining the main causes of discrepancies between different assessments of  
121 the city emission’s impact on its pollution levels and show that these discrepancies generally lead  
122 to underestimating the city's responsibility. It proposes a specific harmonized nomenclature for  
123 source apportionment approaches, and it shows how it is important to document the choices to  
124 enable correct interpretation of the results. We begin with a conceptual overview of the  
125 parameters structuring any SA approach (Section 2). This includes the definition of the key  
126 parameters to any SA study: indicator, source, receptor, and methodology to relate them. Then  
127 (Section 3) we assess the sensitivity of the urban SA results to the choices of these four  
128 parameters. In Section 4, we analyze implications in terms of air quality planning and suggested  
129 strategies. We finally provide conclusions in Section 5.

130 **2. Assessing the city responsibility on air pollution: Main concepts**

131 In this section, we detail the steps required to quantify the responsibility of a city on its air  
 132 pollution, through source apportionment (SA). SA is a methodology that serves to estimate the  
 133 contribution of a given source at a specific receptor for a given indicator (for example the  
 134 concentration of a given pollutant like PM or NO<sub>2</sub>). It involves the following steps (Figure 1):

- 135  
 136 (1) defining a relevant indicator, denoted as (I) to characterize air pollution  
 137 (2) defining the receptor (R) through its spatio-temporal characteristics, i.e. the area ( $\bar{x}_R$ )  
 138 and time period ( $\bar{t}_R$ ) over which the indicator is averaged  
 139 (3) defining the source (S), in our case the city, and its spatio-temporal characteristics,  
 140 i.e. the city area ( $x_s$ ) and time period for which the city responsibility is assessed ( $t_s$ )  
 141 (4) selecting the source apportionment (SA) methodology to capture the processes that  
 142 relate the source to the receptor.

143 Figure 1 summarizes these steps, as well as the nomenclature and symbols used in this work. We  
 144 use this new nomenclature to attach contextual information (i.e. metadata) to the source  
 145 apportionment. Further explanations of the symbols are given in the subsections below.  
 146



147  
 148 *Figure 1: Schematic flow chart representing the four steps required to fully define any SA process. The red letters indicate the*  
 149 *indicator characteristic under consideration. The general notation for the indicator (I) includes a superscript for the*  
 150 *methodological approach (M), a subscript to inform on the source (S) and brackets to inform on the receptor (R). The spatial and*  
 151 *temporal dimensions associated to the source and receptor are denoted by "x" and "t", respectively. The overbar indicates an*  
 152 *averaging process. The lowest row provides for each parameter examples used in this work. Some images used in this schematic*  
 153 *flow chart are adapted from flaticon.com.*

154 **2.1 Definition of the air pollution indicator (I)**

155 The first step required to assess the role/responsibility of city emissions with respect to its air  
 156 pollution, is to define an indicator that identifies the pollution aspect we are interested in. The  
 157 indicator can be defined in many ways. For example, as the total concentration of a given  
 158 compound (e.g. PM), or as a specific constituent of that total concentration (e.g. PM<sub>2.5</sub> or its

159 primary fraction, PPM), or as a composite based on a mix of different pollutants (e.g. maximum  
 160 among O<sub>3</sub>, PM<sub>2.5</sub> and NO<sub>2</sub> concentrations as in some air quality indexes such as ATMO2003) or  
 161 as population exposure (i.e. product of population and concentration).

## 162 2.2 Definition of the receptor (R)

163 Estimating the indicator, either from a measuring instrument or from a model simulation, implies  
 164 an averaging process, both in space and time. For model data, averages correspond to the spatial  
 165 and temporal resolutions (e.g. the time step and grid cell size) whereas for measurement, the  
 166 space-time average will depend on the instrument acquisition time and on the atmospheric  
 167 dispersion characteristics at the measuring site. Regardless of these intrinsic time and space  
 168 averages, indicators are generally averaged over longer spatial and temporal scales for  
 169 convenience. The receptor is defined as the spatio-temporal entity over which the indicator is  
 170 averaged. Both a spatial and a temporal scale (denoted by  $\bar{x}_r$  and  $\bar{t}_r$ , respectively) must be  
 171 associated to the receptor to define it.

172  
 173 For the temporal dimension, typical examples for PM<sub>2.5</sub> are days ( $\bar{t}_r = \bar{D}$ ) or years ( $\bar{t}_r = \bar{Y}$ ).  
 174 Spatially, the indicator can be estimated at a specific location, e.g. the city center ( $\bar{x}_r = \bar{x}_{center}$ ),  
 175 at the location where the maximum concentration occurs ( $\bar{x}_r = \bar{x}_{max}$ ) or averaged over the city  
 176 ( $\bar{x}_r = \overline{city}$ ). For convenience, we use indifferently the following notations to refer to the  
 177 receptor:

$$178 \quad R(\bar{x}_r, \bar{t}_r) = R = \bar{x}_r, \bar{t}_r \quad (1)$$

## 179 2.3 Definition of the source (S)

180 The source is defined as the spatio-temporal entity (e.g. city, emission macro-sector...) for which  
 181 we assess the contribution to the indicator. For the purpose of this work, the source is defined as  
 182 the city, and more precisely as the emissions that originate from a given city. The source  
 183 emissions (denoted by E) are indeed responsible for the pollution fraction that can be associated  
 184 to the source/city at the receptor (R). These emissions are characterized by a spatial ( $x_s =$   
 185 extension of the city) and a temporal scale ( $t_s =$  period of time over which the source activity is  
 186 assessed). For convenience, we use indifferently the following notations to refer to the source:

$$187 \quad S(x_s, t_s) = S = E = city = x_s, t_s \quad (2)$$

188  
 189 In this work, we analyse in particular the impact of the city extension ( $x_s$ ) on the apportionment  
 190 outcome. For this purpose, we define cities in two ways:

- 191  
 192 (1) as core cities, i.e. the local administrative units, with a population density above  
 193 1500/km<sup>2</sup> and a population above 50,000, where the majority of the population lives in an  
 194 urban center and  
 195 (2) as functional urban areas (OECD, 2012, denoted as “FUA”) composed as core cities plus  
 196 their wider commuting zone, consisting of the surrounding travel-to-work areas where at  
 197 least 15% of the employed residents work in the city.

198 Details on the FUA and core city areas are available for 150 EU cities in the urban PM<sub>2.5</sub> atlas  
 199 (Thunis et al. 2017). Note that other city definitions exist. In the context of the CAMS source  
 200 allocation analysis, city are defined as an arbitrary number of grid cells in the modelling domain  
 201 (Pommier et al., 2020).

202 Finally, we define the city background as the sum of all contributions from sources that are not  
 203 covered by the spatial ( $x_s$ ) and temporal ( $t_s$ ) scales of the city source.

204  
 205 One main difference between sources and receptors is that for the latter, spatio-temporal  
 206 characteristics are averaged. Apart from this, temporal and spatial characteristics can also differ  
 207 in terms of value. For example, the source can be defined as the FUA ( $x_s = \text{FUA}$ ) while the  
 208 receptor is a specific location ( $\bar{x}_r = \bar{x}_{max}$ ). Temporally, interest can be on assessing the  
 209 contribution of the city weekly activity ( $t_s = 1$  week) for a given day ( $\bar{t}_r = \bar{D}$ ) at the receptor. In  
 210 the results presented here, the source and receptor temporal scales are however chosen identical  
 211 for convenience.

## 212 2.4 Selection of the SA methodology

213 When the air pollution indicator and the spatio-temporal characteristics of both the receptor and  
 214 the source have been selected, the next step consists in distinguishing and quantifying the  
 215 fractions of the indicator related to the city source ( $I_{city}(R)$ ) and to the background ( $I_{bg}(R)$ ) at  
 216 receptor R, respectively. This decomposition is summarized by the following equation:

$$217 \quad I(R) \rightarrow \{I_{city}(R), I_{bg}(R)\} \quad (3)$$

218  
 219 Different SA methodologies exist to perform this operation. In this section, we describe three  
 220 main approaches but only in brief, as details about each of these are discussed in other works  
 221 (Clappier et al. 2017; Thunis et al., 2019, 2018; Mertens et al. 2018). As mentioned previously,  
 222 we use the indicator's superscript to refer to its calculation method [ $I_{city}^M(R)$ ]. Methods are  
 223 summarized in Table 1.

224  
 225 Potential impacts (PI): The city contribution in this method is denoted as  $I_{city}^{PI100}(R)$  and is  
 226 calculated as the difference between two simulations: a base-case that includes the city  
 227 [ $I(R)$ ] and a scenario in which the city emissions are switched off [ $I_{city}^{100}(R)$ ]. In this notation,  
 228 the source superscript (here, 100) indicates the percentage intensity by which the source  
 229 emissions are reduced. Reductions are intended as percentage variations from the base-case  
 230 situation. The same approach can be used with reduction percentages that are lower than 100%.  
 231 In this case the resulting difference is divided by the reduction percentage to obtain the potential  
 232 impact ( $I_{city}^{PI\alpha}(R)$ ). A similar approach is used to calculate the background contribution, i.e. by  
 233 removing or reducing partially the background emission sources. Potential impacts methods for  
 234 source apportionment are widely used (Osada et al. 2009; Huszar et al. 2016, Huang et al. 2018;  
 235 Wang et al. 2014; Wang et al. 2015; Van Dingenen et al. 2018; Thunis et al. 2016; Clappier et al.  
 236 2015; Pisoni et al. 2017).

237  
 238 Increment (INC): With this methodology, the background contribution is estimated as the  
 239 concentration observed/modelled at a given location "y" [ $I_{bg}^{INC}(R) = I(\bar{y}, \bar{t}_r)$ ]. This location must  
 240 be far enough from the source, not to feel its influence but be close enough to the source to avoid

241 influences from other sources, external to the city. These assumptions are further described and  
 242 discussed in Thunis et al. (2017). The city contribution is then obtained as the difference between  
 243 the base case indicator and the background contribution [ $I_{city}^{INC}(R) = I(\bar{x}_r, \bar{t}_r) - I(\bar{y}, \bar{t}_r)$ ]. The  
 244 increment methodology has been used e.g. by Lenschow et al. (2001), Petetin et al. (2014),  
 245 Kiesewetter et al. (2015), Squizzato et al. 2015, Timmermans et al. 2013, Keuken et al. 2013,  
 246 Ortiz and Friedrich 2013 and Pey et al. 2010.

247  
 248 **Tagging (TAG):** With this approach, species emitted by the city are numerically tagged and  
 249 followed through the modelled transport, dispersion and chemical transformation processes.  
 250 When chemical transformations take place, preserved atoms are used as tracers. For example, the  
 251 nitrogen atom (N) will be used to follow the NO source emissions through its successive  
 252 transformations into NO<sub>2</sub> and HNO<sub>3</sub> to reach its final product NO<sub>3</sub>, that will then be attributed to  
 253 that source. Example of tagging applications are e.g. Kranenburg et al. 2013, Yarwood et al.  
 254 2004; Wagstrom et al., 2008; Kwok et al. 2013; Bhave et al. 2007; Wang et al., 2009. Some of  
 255 these approaches are implemented operationally to estimate daily city contributions on air  
 256 pollution (<https://topas.tno.nl/documentation/>). The formulations corresponding to these three  
 257 main approaches are summarized in Table 1.

258  
 259 A few key points are worth noting. While tagging and potential impacts approaches explicitly  
 260 consider city emissions in their calculations, this is not the case for increments that only refer to  
 261 them implicitly. By construction, both the increment and tagging approaches are additive [i.e.  
 262  $I(R) = I_{city}(R) + I_{bg}(R)$ ] whereas this is not the case for potential impacts when pollutants  
 263 behave non-linearly because of air transport, deposition or chemical processes (Clappier et al.,  
 264 2017).

265  
 266

	<b>City contribution</b>	<b>Background contribution</b>
<b>Potential Impact</b>	$I_{city}^{PI\alpha} = \frac{I(R) - I_{city\alpha}(R)}{\alpha}$	$I_{bg}^{PI\alpha} = \frac{I(R) - I_{bg\alpha}(R)}{\alpha}$
<b>Increment</b>	$I_{city}^{INC} = I(\bar{x}_r, \bar{t}_r) - I(\bar{y}, \bar{t}_r)$	$I_{bg}^{INC} = I(\bar{y}, \bar{t}_r)$
<b>Tagging</b>	$I_{city}^{TAG} = \sum_E^{city} I_E(R)$	$I_{bg}^{TAG} = \sum_E^{bg} I_E(R)$

267 *Table 1: Formulation of the three main methods to estimate the contribution/impact/increment of a city. The letters, I, S and R*  
 268 *refer to the indicator, source and receptor, respectively. The indicator superscript refers to the SA method (PI for potential*  
 269 *impacts, INC for increments and TAG for tagging) while its subscript indicates the source (city or background (bg)).  $\alpha$  represents*  
 270 *the percentage reduction factor applied for the source emissions in the potential impacts method. See text for additional details.*

### 271 3. Results

272 Recognizing the impossibility of assessing the sensitivity of the results for all combinations of  
273 indicators, source, receptor and methodology, we focus our analysis on comparisons in which  
274 only one parameter is changed at a time, to highlight major sensitivities. For this purpose, we use  
275 the following two main sources of data and results.

- 276 • SHERPA: SHERPA is a modelling tool, based on Source-Receptor Relationships that  
277 represent a simplified version of a Chemistry Transport Model, used to simulate the  
278 contribution to PM<sub>2.5</sub> concentration levels by all precursor emissions (NO<sub>x</sub>, NMVOC,  
279 PPM, SO<sub>2</sub> and NH<sub>3</sub>) from different cities in Europe (Clappier et al. 2015, Thunis et al.  
280 2016, 2018). In its current configuration, SHERPA is based on the CHIMERE model  
281 (Menut et al. 2013) covering the whole of Europe at roughly 7 km spatial resolution. In  
282 this work, we use the source apportionment results over 150 cities as reported in the  
283 PM<sub>2.5</sub> urban atlas (Thunis et al., 2017) as well as additional SHERPA data to provide  
284 further analysis.
- 285 • EMEP simulations: The EMEP model is an off-line regional transport chemistry model  
286 (Simpson et al., 2012; <https://github.com/metno/emep-ctm>). The model has 20 vertical  
287 levels, with the first level around 50 m. The model uses meteorological initial conditions  
288 and lateral boundary conditions from the European Centre for Medium Range Weather  
289 Forecasting (ECMWF-IFS). The meteorological year is 2015. Detailed information on  
290 the meteorological driver, land cover, model physics and chemistry are described in  
291 Simpson et al. (2012) and in the EMEP Status Report 2017  
292 ([https://emep.int/publ/reports/2017/EMEP\\_Status\\_Report\\_1\\_2017.pdf](https://emep.int/publ/reports/2017/EMEP_Status_Report_1_2017.pdf)). In this work, we  
293 use specific simulations where emissions have been removed partially or fully in a series  
294 of European cities. Additional details regarding these simulations are provided together  
295 with the discussion of the results.

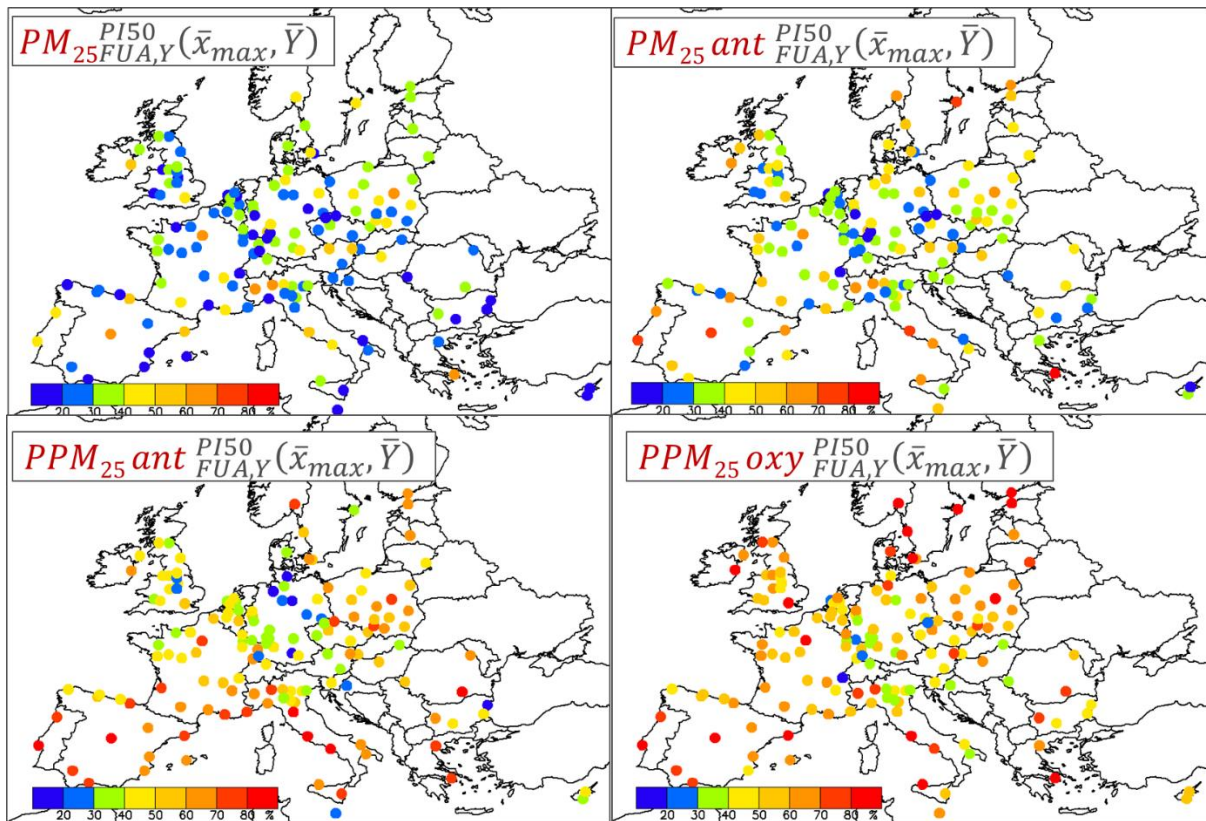
296 Based on these sources of information and data, we discuss hereafter the sensitivity of the SA  
297 results to the choice of the indicator (Section 3.1), to the choice of the methodology (Section  
298 3.2), to the source (Section 3.3) and finally to the receptor (Section 3.4).

#### 301 3.1 Sensitivity to the indicator

302 The implications resulting from the choice of the indicator are illustrated in Figure 2 for four  
303 indicators, based on SHERPA results for 150 cities in Europe. The four indicators selected to  
304 characterize air pollution are: a) the PM<sub>2.5</sub> concentration (top left, from Thunis et al. 2017), b) the  
305 anthropogenic fraction of PM<sub>2.5</sub> (“PM<sub>2.5</sub> ant”, top right), c) the primary anthropogenic fraction of  
306 PM<sub>2.5</sub> (“PPM<sub>2.5</sub> ant” bottom left) and d) the primary fraction of PM<sub>2.5</sub> originating from the  
307 transport and residential sectors (“PPM<sub>2.5</sub> oxy”, bottom left). The reference (PM<sub>2.5</sub> total mass, top  
308 left) corresponds to the indicator currently used in legislation (e.g. European Ambient Air  
309 Quality Directive, AAQD2008) against which health impacts are correlated (WHO2005). In the  
310 second case, the indicator is limited to its anthropogenic fraction (PM<sub>2.5</sub> ant), excluding therefore  
311 natural contributions (dust, marine salt...). This is motivated by the fact that policies have no  
312 impact on this component. According to this indicator, city contributions increase significantly



313 (by about 20% in average) and in some cities where natural dust pollution is important (e.g. in  
 314 Sicily), the city responsibility shifts from minor to major. If we further restrict the indicator to its  
 315 primary anthropogenic fraction (“PPM<sub>2.5 ant</sub>”, bottom right) because of its suggested higher  
 316 health burden (Park et al., 2018; Viana et al., 2008), the city contribution then increases  
 317 significantly in most cities. This becomes even more striking if we limit the indicator to the  
 318 PPM<sub>2.5</sub> fraction originating from the transport and residential sectors (bottom right). These two  
 319 sectors have recently been shown to generate the largest burden on human health given the high-  
 320 oxidative potential of their emissions (Rankjar et al., 2020, Li et al. 2016). With this indicator,  
 321 the majority of EU cities become main contributors to their pollution. Regarding the latter  
 322 indicator, it is important to note that although the increasing adoption of electric vehicles shows  
 323 rather positive impacts on health (Choma, 2020), the remaining PM emissions from road traffic  
 324 like tires and brake and road wear emissions (Kole et al., 2017; EC, 2014; Ntziachristos and  
 325 Boulter, 2019) will remain an issue. The calculation of various geochemical indices (enrichment  
 326 factor, geo-accumulation index, pollution index and potential ecological risk) also show that road  
 327 dust is extremely enriched and contaminated by elements from tire and brake wear (e.g. Sb, Sn,  
 328 Cu, Bi and Zn).  
 329



330  
 331 Figure 2: SHERPA results for 150 major cities in Europe for the overall PM<sub>2.5</sub> concentration (top left), for its anthropogenic  
 332 fraction (“PM<sub>25\_ant</sub>”, top right), for its anthropogenic primary fraction (“PPM<sub>25\_ant</sub>”, bottom left) and for its primary  
 333 fraction originating from the transport and residential sectors (“PPM<sub>25\_ox</sub>”, bottom right). For all cities, the source is defined  
 334 spatially as the FUA over which emissions are reduced over a year (Y). The receptor is defined as the city location where the  
 335 concentration is maximum ( $\bar{x}_{max}$ ) and the indicator is averaged yearly at the receptor ( $\bar{Y}$ ). All calculations are made with the  
 336 same SA methodology, namely, potential impacts (PI) with city emissions reduced by 50% (PI50)

## 337 3.2 Sensitivity to the SA methodology

338 A comparison of SA methodologies is proposed in Thunis et al. (2019) where the potential  
339 impact, increment and tagging approaches are compared both on simple theoretical examples and  
340 on real data to highlight differences among methods and stress their limitations. In this section,  
341 we summarize the main findings of this work and complement it with comparisons that focus on  
342 the apportionment of the city vs. background contributions. We also provide in the appendix a  
343 comparison of all SA methods discussed in this section, applied on a theoretical example tuned  
344 to the city scale.

### 345 Increment vs. potential impacts

346 Thunis (2017) compared increments and potential impacts with the SHERPA model for a series  
347 of European cities. He showed that increment approaches lead to important underestimations (30  
348 to 50%) of the city responsibility for PM<sub>2.5</sub> and NO<sub>2</sub> with respect to potential impacts. This  
349 underestimation is explained by the non-fulfilment of the two underlying increment assumptions,  
350 related to the external location [i.e.  $y$  in  $I_{bg}^{INC}(R) = I(\bar{y}, \bar{t}_r)$ ] that must: 1) be far enough from the  
351 city, not to feel its influence but 2) close enough to the city to avoid influences from sources  
352 external to the city. The Author show that these two assumptions are seldom fulfilled in reality.  
353

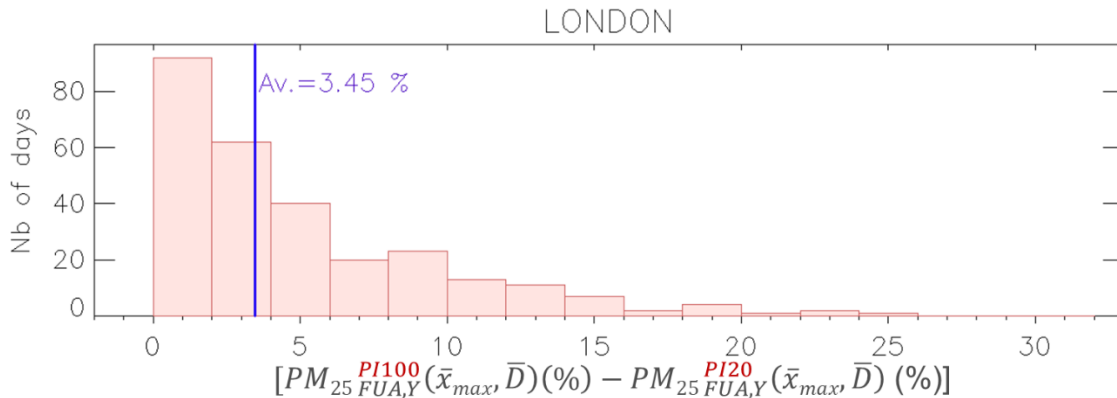
### 354 Tagging vs. potential impacts

355 Clappier et al. (2017) discussed the concepts underlying these two SA methods and showed that  
356 important differences in terms of results arise as soon as non-linear processes are present. Belis  
357 et al. (2020) highlighted and quantified these large differences based on a real-case inter-  
358 comparison exercise. Finally, Thunis et al. (2019) reviewed in their work many inter-  
359 comparisons between tagging and potential impact SA results. In their application over the Po  
360 basin (Italy), they showed that differences are large for the agriculture sector (dominated by NH<sub>3</sub>  
361 emissions) but are also important for other sectors, when dealing with high temporal resolution  
362 (e.g. daily) at the receptor. Unfortunately, these examples did not address the particular case of a  
363 city scale apportionment.  
364

### 365 Full vs. partial potential impacts

366 To analyze differences between full and partial impacts, we use a series of EMEP simulations in  
367 which we remove totally (PI100) or partly (PI20) the London FUA emissions (source) during an  
368 entire year. Figure 3 shows the differences between city contributions obtained with the two PI  
369 methods. Differences can be important (up to 25 percentage points for specific days). Although  
370 the number of high-difference days is limited (leading to a yearly average difference of few  
371 percents), these days might represent high pollution episodes for which assessing the city  
372 responsibility is important to act. In general, the higher resolution applied to the temporal and/or  
373 spatial averages at the receptor, the largest the differences are among methods. It is also  
374 interesting to note that partial potential impacts systematically underestimate full potentials (no  
375 negative values).  
376

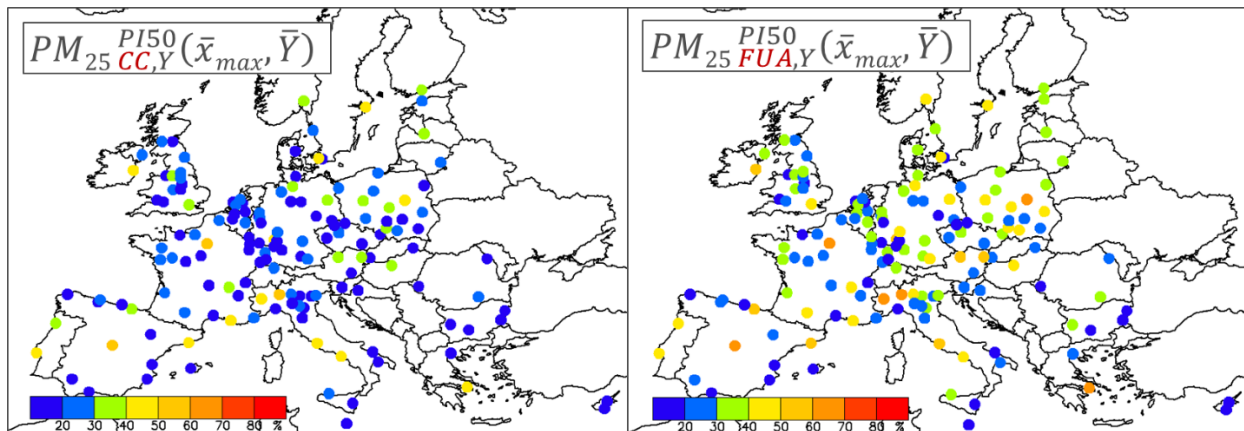
377  
378  
379  
380



381  
 382 *Figure 3: Histogram of daily city contribution differences to London  $PM_{2.5}$  levels between two potential impacts methods, PI100*  
 383 *and PI20, calculated with the EMEP model. The source is defined spatially as the FUA where emissions are reduced yearly (Y*  
 384 *subscript). The receptor is defined as the city location where the maximum yearly averaged concentration is modelled ( $\bar{x}_{max}$ ),*  
 385 *and temporally as daily average ( $\bar{D}$ ). Each column represents the number of days with a specific PI difference (PI100 - PI20). The*  
 386 *blue line provides the yearly average difference.*

### 387 3.3 Sensitivity to the source

388 Figure 4 shows the comparison between SA obtained with sources defined as core cities (left)  
 389 and as FUA (right). The city contribution / responsibility is multiplied by a factor 2 on average  
 390 (see also Figure 8) when FUA are considered. The larger spatial extension of the FUA and its  
 391 implied additional emissions explain the differences that lead some cities to become a major  
 392 actor, i.e. where the city contribution dominates the background one (e.g. Athens, Warsaw,  
 393 Milan, Turin and Rome).  
 394



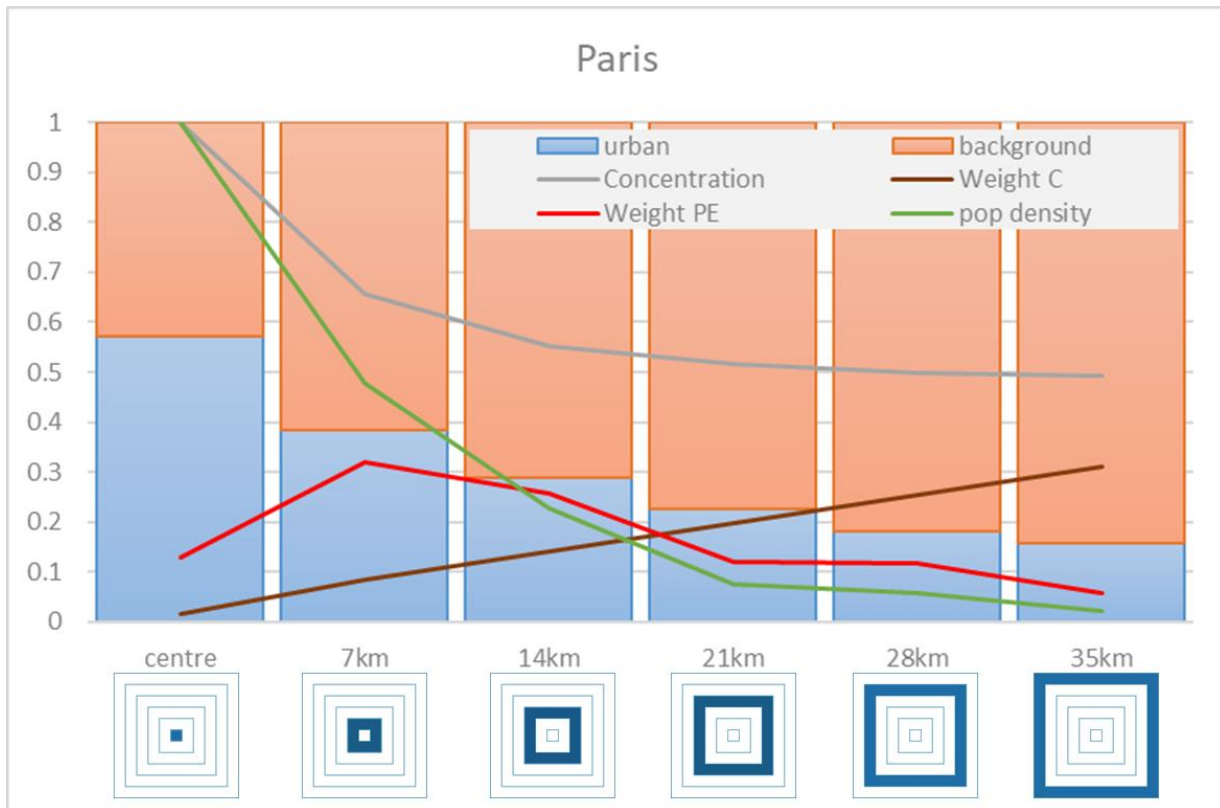
395  
 396 *Figure 4: Maps of city contributions obtained for spatial sources defined in 2 ways: core city (CC, left) and FUA (right). Results are*  
 397 *shown for 150 cities in Europe, based on the SHERPA-CHIMERE model using a potential impact SA method for a reduction*  
 398 *strength of 50% (PI50). The indicator is the total  $PM_{2.5}$  concentration. The receptor is selected as the location where the*  
 399 *maximum yearly average concentration occurs ( $\bar{x}_{max}$ ) and applies yearly time average ( $\bar{Y}$ ). The source emissions are reduced*  
 400 *over a full year (Y).*

### 401 3.4 Sensitivity to the receptor

402 In this section, we discuss the spatial and temporal averages applied at the receptor. Spatially,  
 403 different averaging options exist, ranging from a single location (i.e. one model grid cell) to more  
 404 or less extended areas covering part of the source or even larger. To illustrate the sensitivity of

405 SA to that choice, we use the case of Paris (Figure 5) where emission have been reduced over the  
 406 FUA (source) over a full year.

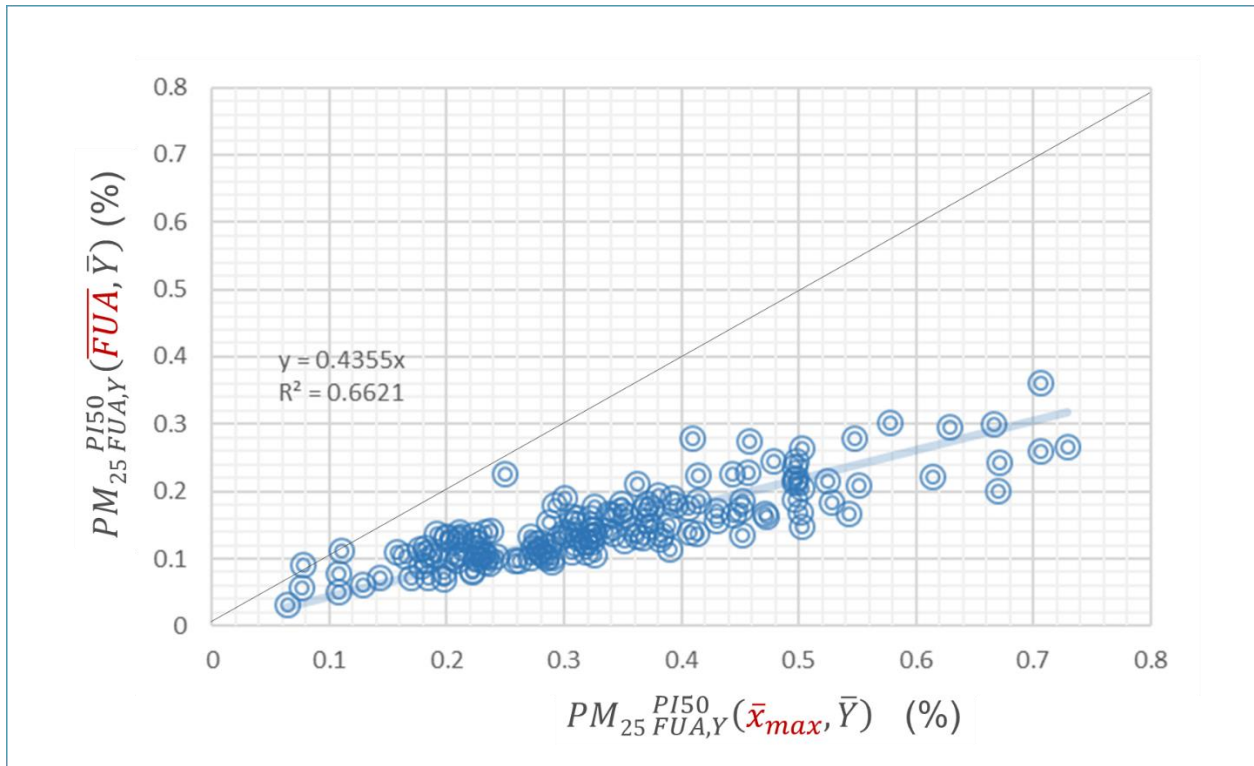
407  
 408 SA varies largely from one location to another within Paris. We highlight this with bars that  
 409 distinguish the city vs. background contributions for locations at different distance from the city  
 410 centre. We note opposite trends, dominated by the city source (around 60%) at the city center  
 411 and dominated by the background source towards the periphery (around 80%). While the SA at  
 412 the city centre is representative of a single cell within the city, this is not the case for SA close to  
 413 the periphery. This is highlighted by the city rings (below the X-axis) that indicate the area of  
 414 representiveness of a given SA. When we average spatially an indicator ( $PM_{2.5}$  or population  
 415 exposure) over a receptor that covers the entire FUA (all 6 rings), these areas of  
 416 representiveness enter into play. The brown curve indicates the weight (in the spatial average)  
 417 attached to each city ring, relatively to the city total (i.e. all rings). Weights increase fast when  
 418 moving towards the periphery because of the larger ring areas. The spatial averaging process  
 419 leads to over-representing the periphery, which overweight the city center SA by almost a factor  
 420 40. It is interesting and counter-intuitive to note that with this averaging process, the city  
 421 responsibility decreases when the city area increases. With population exposure as indicator  
 422 (weights shown by red curve), the rapid population density decrease balances the ring area  
 423 increase when moving outward, leading to weights that dominate for middle rings. With average  
 424 population exposure, the city center weight is yet similar to the weight obtained 28 km away.  
 425



426  
 427  
 428  
 429  
 430  
 Figure 5: City rings' source apportionment for Paris  $PM_{2.5}$  and associated population exposure. The city/background apportionment (bars) is represented for rings (i) progressively more distant from the city centre (X axis). The ring average concentration ( $C_i$ ) and population density ( $P_i$ ) relative to the city centre values are represented in blue and green, respectively. The relative (to the FUA total, i.e. all rings) weight of each ring (i) in the city average concentration (brown) is calculated as

431  $C_i * S_i / \sum_i (C_i * S_i)$  where  $S_i$  is the ring area, respectively. A similar expression:  $C_i * S_i * P_i / \sum_i (C_i * S_i * P_i)$  is used to determine  
 432 the weight of each ring in the calculation of the average population exposure (red curve).

433 Figure 6 compares SA for 150 cities obtained for receptors defined (1) as the location where the  
 434 maximum concentration is reached within the FUA ( $\bar{x}_{max}$ ) and (2) as the FUA spatial average  
 435 ( $\bar{FUA}$ ). In average, city impacts for a spatially averaged receptor are about 55% lower.  
 436 Depending on the spatial characteristic of the receptor, some cities will be considered as minor or  
 437 major actors with respect to their pollution. We discuss this point further in Section 4.  
 438



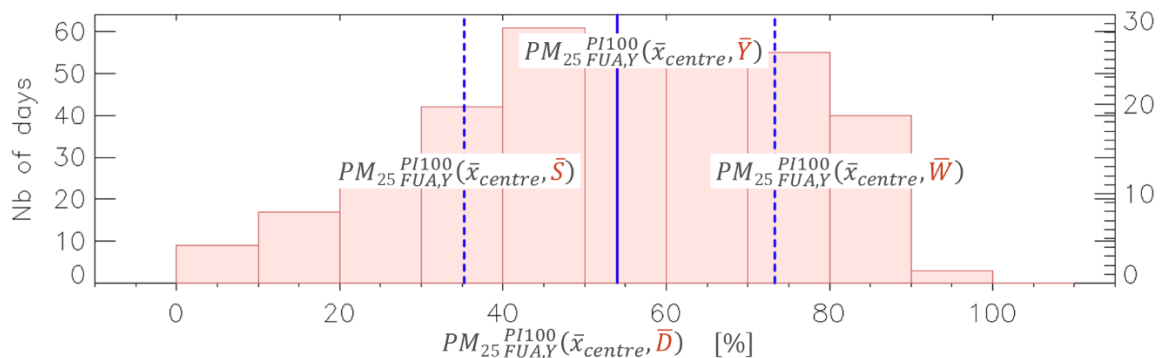
439  
 440 Figure 6: Comparison of potential impacts for 150 cities in Europe obtained for a receptor spatially defined as the location where  
 441 the concentration is maximum in the city ( $\bar{x}_{max}$  – X axis) and defined as the FUA spatial averaged ( $\bar{FUA}$ ). For these calculations,  
 442 the source are defined as the FUA over which emissions are switched off during the whole year. The indicator is the total  $PM_{2.5}$   
 443 mass. All results are based on the SHERPA-CHIMERE model using a potential impact SA method for a reduction strength of 50%  
 444 ( $PI50$ ) and are based on yearly averages at the receptor ( $\bar{Y}$ ).

445 As seen from these results, spatial averages at the receptor significantly reduce the city  
 446 responsibility, potentially leading to underestimating the city ability to reduce pollution levels  
 447 via local controls. The large differences resulting from the choice of the receptor settings prevent  
 448 meaningful comparisons. It is for example challenging to compare CAMS city contributions that  
 449 are averaged spatially over the city area with the urban results obtained in the context of the  
 450 Thematic Strategy on Air Pollution (Kiesewetter and Amann 2014) that are aggregated at  
 451 country level or with SHERPA estimates based on a single grid cell receptor. It is therefore  
 452 crucial to associate all SA settings (metadata) to the results in order to inform on the  
 453 meaningfulness of a comparison. We discuss further this issue in the context of air quality  
 454 planning in Section 4.  
 455

456 Similar considerations apply to temporal averages. Figure 7 compares SA obtained when the  
 457 indicator at the receptor is averaged yearly and seasonally with daily single values. For a yearly  
 458 average, Madrid city's contribution is 54% but the spectra of daily contributions show variations  
 459 that range from 10 to beyond 90%. Even seasonal averages show important differences with a  
 460 factor 2 between summer and winter. Similarly, to spatial averages, temporal averages  
 461 encompass a large spectra of SA outcome. Indicators averaged yearly at the receptor have been  
 462 used for example in SHERPA (Thunis et al. 2017), GAINS (Kiesewetter and Amann, 2014)  
 463 whereas daily indicators are used in CAMS (Pommier et al., 2020). Correlating low and high  
 464 city contributions to meteorological factors (cold vs warm days, windy vs calm situations...) is  
 465 beyond the scope of this work. This point is however addressed in Pisoni et al. (2021).

466  
 467 Note that spatial averages have a larger smoothing effect than temporal ones because they are  
 468 bidimensional.

469



470

471

472

473

474

Figure 7: Frequency histogram of daily potential impact at 100% (PI100) modelled with the EMEP model for the city of Madrid. Each column represents the number of days with a given daily PI. The blue line provides the yearly average PI. For these calculations, the source is the Madrid Functional Urban Area (FUA) over which emissions are switched off during the whole year (Y). The indicator is the total PM<sub>2,5</sub> mass. The receptor point is the city centre location ( $\bar{x}_{centre}$ ).

### 475 3.5 Methodological assumptions and uncertainties

476 In addition to referring to the SA method itself (Section 2.4), other modelling parameters need to  
 477 be documented as well. We list hereafter the main ones.

478

479 One of the main assumption attached to models is the spatial resolution and its potential impact  
 480 on the calculation of the city contribution. While a coarse resolution might be able to capture  
 481 relatively well the background (characterized by smoother fields), this will not be the case for  
 482 peak concentrations within the city. The coarser the model spatial resolution, the largest the  
 483 underestimation of the city responsibility will be (De Meij et al., 2007).

484

485 Uncertainties may result from our incomplete knowledge of some model input parameters, in  
 486 particular chemical processes and emission sources. Some urban emission sources are not well  
 487 documented and are probably underestimated. This is the case of residential emissions for which  
 488 the inclusion of condensable remains a question mark (Bessagnet and Allemand, 2020, Simpson  
 489 et al., 2020) or for the resuspension of particles generated by vehicles (Amato et al., 2014). On  
 490 the other hand the spatial allocation for emissions can be uncertain for some sectors. These  
 491 lacking or incomplete emission sources will lead to a potential misestimate of the city  
 492 responsibility.

493  
494 On the meteorological side, the estimation of wind speed, PBL height and/or turbulence intensity  
495 will largely influence the dispersion of city emissions and uncertainties in these will therefore  
496 impact the calculation of city contributions. While the impact of meteorological parameterization  
497 on air quality has been extensively assessed from regional to urban cases (De Meij et al., 2009;  
498 (De Meij et al. 2015; De Meij et al, 2018; Jiang et al., 2020), only few studies assessed their  
499 importance on city contributions. One of these (Huszar et al. 2021) shows e.g. that the inclusion  
500 of an urban canopy meteorological forcing on multi-year simulations largely impacts the  
501 estimation of the city responsibility. In the next section, we discuss the consequences of these  
502 results on policy, in particular when SA information is used to design air quality plans.

#### 503 4. Implications for air quality strategies

504 Estimating the contribution of a city to its pollution has important consequences in terms of air  
505 quality management. Indeed, an important city contribution will be a logic argument to support  
506 substantial control measures at the local level to abate pollution. The effectiveness of the control  
507 measures then relies on the relevance and accuracy of this city contribution; over- or under-  
508 estimated city contributions potentially leading to inefficient measures.

509 In previous sections, we have seen that the city contribution largely varies depending on the  
510 choices made for the SA setting parameters (definition of the indicator, source, receptor and  
511 methodology), hence the challenge to obtain a relevant and accurate estimate to support local  
512 action.

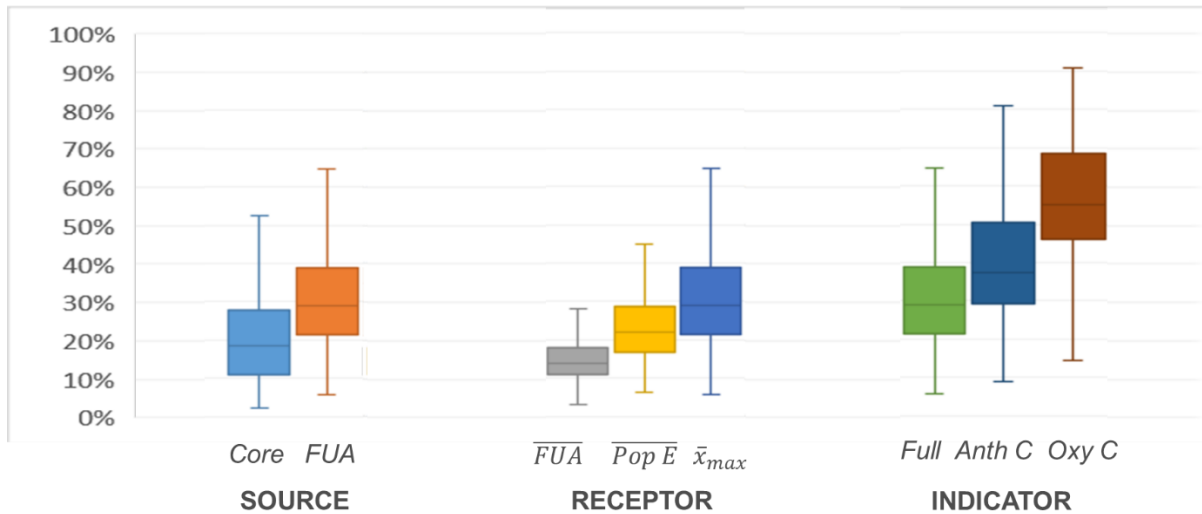
513 Given the range of possible SA options and their impact on results, the first recommendation is  
514 obviously to report these SA setting choices together with the results to provide policymakers  
515 with the full picture and allow them to take informed decisions. This advocates for the use of the  
516 proposed nomenclature or a similar one that documents for the choices in the SA approach,  
517 providing accountability to the method and enabling correct interpretation of the results. The  
518 proposed nomenclature can be understood as a documentation of the SA metadata information.  
519 Apart from this point on the importance of documenting SA approach choices, we show below  
520 that some of the SA settings are fixed by the purpose of the study. We provide suggestions for  
521 the remaining free choices.

#### 522 523 The recommended SA method is potential impacts (PI)

524 It is important to recall that not all SA methodologies are equally suited to support air quality  
525 planning. As mentioned by several authors (Burr and Zhang 2011, Qiao et al. 2018, Mertens et  
526 al. 2019, Clappier et al. 2017, Grewe et al. 2010, 2012; Thunis et al. 2019), potential impacts are  
527 recommended when non-linear species are involved (which is the case for PM<sub>2.5</sub> and PM<sub>10</sub> but  
528 also for other species like NO<sub>2</sub> or O<sub>3</sub>). It is worth reminding that tagging or incremental  
529 approaches are yet erroneously used and believed to be suited for air quality planning purposes  
530 (Qiao et al. 2018; Guo et al. 2017; Itahashi et al. 2017; Timmermans et al. 2017; Wang et al.  
531 2015, Hendriks et al. 2013). Although challenging practical issues are attached to potential  
532 impacts and may be seen as a burden (e.g. lack of additivity, see Appendix), they only reflect the  
533 complexity of the real processes that must be accounted for. It is true that uncertainties  
534 associated to the PI approach (e.g. imperfect emission inventory), may lead other SA methods to  
535 perform better in some instances because methodological biases compensate uncertainties, this is  
536 however coincidental. While uncertainties can be tackled and reduced to improve the approach,

537 this is not the case of methodological biases. These points are extensively discussed in Thunis et  
 538 al. (2019).

539  
 540 For the remaining of this section focusing on policy aspects, only potential impact results are  
 541 discussed. Fixing the methodology however still leaves free options in terms of indicator,  
 542 receptor and source. This is visualized in Figure 8 that summarizes the variability of the SA  
 543 results presented in the previous sections (i.e. Figure 2, Figure 4 and Figure 6) for the 150 cities  
 544 to these possible choices. Differences in terms of city responsibility reach a factor 2 in average  
 545 for each of these remaining parameters with much larger values for some cities.  
 546



547  
 548 *Figure 8: Box quantile diagrams summarizing the city contributions to PM<sub>2.5</sub> levels for the 150 EU cities. All results are based on*  
 549 *a similar method (potential impacts at 50%), a similar temporal receptor ( $\bar{Y}$ ) but for different choices of city sources (left),*  
 550 *receptors (centre) and indicators (right). See previous sections for details. The two extremities of each vertical line represent the*  
 551 *10<sup>th</sup> and 90<sup>th</sup> percentile contributions among the 150 cities, respectively. The box crossing horizontal line represents the median.*

552  
 553 **INDICATOR: The indicator choice is driven by health and environmental objectives**  
 554 The choice of the indicator is generally motivated by health or environmental considerations.  
 555 Currently, the WHO guidelines (WHO2005) refer to the total PM<sub>2.5</sub> mass as the indicator  
 556 correlating best with health impacts. These guidelines (or the AAQD limit values) are then the  
 557 logical and most relevant indicator choice among the options presented in Section 3.1 and shown  
 558 in Figure 2. As illustrated by Figure 8, evolving knowledge on health-related pollution impacts  
 559 (i.e. the increased toxicity of some PM<sub>2.5</sub> constituents like those related to the traffic and  
 560 residential activities) might however drive the choice towards more detailed indicators (e.g.  
 561 PPM<sub>2.5</sub>) leading to an increased responsibility for the cities.  
 562

563 **SOURCE: Importance of matching sources with governance levels**

564 Figure 8 shows that plans limited to city cores would be significantly less efficient than if applied  
 565 at the FUA scale. In average over all cities, the efficiency decreases by a factor 2 but larger  
 566 differences occur in many cities. The source does however not represent a free choice in the  
 567 context of policy practice. Indeed, authorities in charge of AQ plans only have power to act on  
 568 the area under their responsibility, which sets where measures apply. The same applies for the  
 569 source temporal characteristic, fixed as the period of time during which measures apply. A good



570 match between the SA settings and the temporal and spatial characteristics of the source is  
571 therefore important to provide meaningful support to policy makers.

572  
573 RECEPTOR: Drawbacks associated to spatial and temporal averaging processes at the receptor

574 As clearly shown in Figure 5, spatial averaging processes lead to a loss of information. In our  
575 example, a city average based SA would totally occult the city center SA. It would lead to a  
576 strategy that mostly targets the background at the expense of the city center, where the high  
577 concentration issues would not be solved. This is well illustrated by Amann et al. (2017) who  
578 analyze the responsibility of the city of New Delhi on its air pollution, both at a city center hot-  
579 spot receptor and in terms of city average population exposure. In the first case, SA suggests  
580 acting on local sources while in the second SA suggests acting on regional sources. Spatial  
581 averaging drives the balance towards regional actions that will be less effective in solving the  
582 pollution issue at the city center. The larger the city, the more important this shift will be. As  
583 illustrated by Figure 8, there is more than a factor 2 between city-averaged and hot spot  
584 indicators. Similar considerations apply to temporal averages. Figure 7 clearly shows that yearly  
585 average values hide the potential for effective local actions during wintertime and even more on  
586 specific days.

587  
588 Averaging implies merging, into one single number, locations and time instants that are  
589 characterized by different and sometimes opposite SA. This may lead to strategies that will not  
590 be efficient everywhere all the time. Whenever the final objective is to reduce a temporally  
591 or/and spatially averaged indicator (e.g. average population exposure), strategies would gain in  
592 efficiency with the following process: (1) perform SA and hierarchize the raw (not averaged) SA  
593 results into homogeneous spatio-temporal clusters; (2) design strategies on the basis of these  
594 clusters; (3) assess the strategy efficiency against the averaged indicator. The key is here to  
595 design strategies on raw or clustered results rather than on averaged ones, to prevent information  
596 loss. Note that designing a unique strategy based on multiple SA results (point 2 above) does not  
597 necessarily complicate the analysis, as these different SA will likely suggest action on different  
598 sectors of activity that can be combined in the final strategy.

## 599 5. Conclusions

600 Although air quality has improved in Europe over the last decades, in great part thanks to  
601 effective measures and consistent EU-wide legislation, pollution hot spots yet remain in many  
602 European cities. The extent by which city emissions are causing these elevated urban pollution  
603 levels is however still a subject of scientific discussion. This can be explained by the complex  
604 processes driving the formation of some pollutants like PM<sub>2.5</sub>, for which there is not a simple  
605 relationship between emissions and concentrations (in other words, local emissions don't always  
606 imply local responsibilities). Source apportionment represents a useful technique to quantify the  
607 city responsibility but the approaches and applications are however not harmonized, therefore  
608 not comparable, resulting in confusing and sometimes contradicting interpretations.

609  
610 In this work, we analyzed how different SA approaches apply to the urban scale and how their  
611 building elements and parameters are defined and set. We identified the possible settings  
612 associated to four key steps in SA: indicator, receptor, source and methodology. We showed that  
613 different choices for these settings lead to very large differences in terms of results. In average  
614 over the 150 European large cities selected as example, the choices made for the indicator, the

615 receptor, and the source each lead to an average factor 2 difference in terms of city  
616 responsibility. These various options and the large differences that result, highlight the difficulty  
617 of comparing results from different studies and stress the need to document the SA approach  
618 with its related metadata – that details the choices made for the key four steps.

619  
620 This work advocates for the use of a harmonized nomenclature to support the comparability of  
621 SA approaches. We propose the use of indexes and sub-indexes attached to the 4 key steps in any  
622 SA approach in a harmonized way to uniquely document the approach and enable correct  
623 interpretation of the results. We believe that the adoption of this nomenclature will provide  
624 clarity to the scientific discussion on different results and enable the correct interpretation of the  
625 results for policy applications. Even though this is applied to the specific case of PM<sub>2.5</sub>, the  
626 concepts presented here can easily be generalized to other pollutants.

627  
628 In the context of supporting urban air quality plans, the SA configuration and most setting  
629 parameters are driven by the purpose of the AQ plan itself and by its associated constraints.  
630 While environmental and/or health related considerations guide the choice of the indicator, the  
631 spatio-temporal characteristics of the source are strongly correlated to governance aspects. In  
632 other words, the source characteristics should reflect the governance levels to facilitate  
633 interpretation. Finally, the recommended SA method should be based on “potential impacts”, to  
634 prevent misleading interpretations in terms of expected AQ plan outcome.

635  
636 At the receptor level, temporal and spatial averaging processes lead to a loss of information,  
637 especially when diverging SA results are aggregated into a single number. Averaging process, in  
638 particular spatial, often lead to favor strategies that target background sources while neglecting  
639 actions that would be efficient at the city center. In our 150 cities example, the impact of spatial  
640 averaging leads to an average factor 2 difference in terms of city responsibility. Not only results  
641 differ from one city to the other, and from one location to another in a given city, they also differ  
642 through time. To cope with this variability, we recommend using non-averaged SA results for the  
643 design of AQ strategies. Once clustered in homogeneous spatio-temporal classes, these can serve  
644 to understand where and when actions are most efficient. When implemented, the efficiency of  
645 abatement measures can then be assessed via spatially and temporally averaged indicator (e.g.  
646 city average population exposure).

647  
648 The responsibility of a city to its pollution is obviously city dependent. But even for a given city,  
649 SA studies using different approaches and parameter settings will deliver very different  
650 outcomes. It is important to note that a departure from the methodological recommendations  
651 listed above, additional uncertainties and assumptions will most often lead to a systematic and  
652 important underestimation of the city responsibility. We showed that in average over 150  
653 European cities, departures in terms of source, receptor, and indicator may lead for each to a  
654 factor 2 underestimation. This comes with important implications: if cities are seen as a minor  
655 actor, plans will target in priority the background at the expense of potentially effective local  
656 actions.

657  
658 Future work will consist in comparing spatially/temporally averaged SA results with SA results  
659 that are clustered in homogeneous spatio-temporal classes and assess the implications in terms of  
660 AQ strategy.

661

## 662 Acknowledgements

663 The Authors thank Chloé Thunis for her support in adapting some 'Flaticon.com' images to our  
664 infographics needs.

665

666

## 667 References

- 668 Alberti, V., Alonso Raposo, M., Attardo, C., Auteri, D., Ribeiro Barranco, R., Batista E Silva, F.,  
669 Benczur, P., Bertoldi, P., Bono, F., Bussolari, I., Louro Caldeira, S., Carlsson, J.,  
670 Christidis, P., Christodoulou, A., Ciuffo, B., Corrado, S., Fioretti, C., Galassi, M.,  
671 Galbusera, L., Gawlik, B., Giusti, F., Gomez Prieto, J., Grosso, M., Martinho Guimaraes  
672 Pires Pereira, A., Jacobs, C., Kavalov, B., Kompil, M., Kucas, A., Kona, A., Lavallo, C.,  
673 Leip, A., Lyons, L., Manca, A., Melchiorri, M., Monforti-Ferrario, F., Montalto, V.,  
674 Mortara, B., Natale, F., Panella, F., Pasi, G., Perpia Castillo, C., Pertoldi, M., Pisoni, E.,  
675 Roque Mendes Polvora, A., Rainoldi, A., Rembges, D., Rissola, G., Sala, S., Schade, S.,  
676 Serra, N., Spirito, L., Tsakalidis, A., Schiavina, M., Tintori, G., Vaccari, L., Vandyck, T.,  
677 Vanham, D., Van Heerden, S., Van Noordt, C., Vespe, M., Veters, N., Vilahur  
678 Chiaraviglio, N., Vizcaino, M., Von Estorff, U. and Zulian, G., *The Future of Cities*,  
679 Vandecasteele, I., Baranzelli, C., Siragusa, A. and Aurambout, J. editor(s), EUR 29752  
680 EN, Publications Office of the European Union, Luxembourg, 2019, ISBN 978-92-76-  
681 03847-4, doi:10.2760/375209, JRC116711.
- 682 Amann, M., Pallav Purohit, Anil D. Bhanarkar, Imrich Bertok, Jens Borcken-Kleefeld, Janusz  
683 Cofala, Chris Heyes, Gregor Kiesewetter, Zbigniew Klimont, Jun Liu, Dipanjali  
684 Majumdar, Binh Nguyen, Peter Rafaj, Padma S. Rao, Robert Sander, Wolfgang Schöpp,  
685 Anjali Srivastava, B. Harsh Vardhan, 2017. *Managing future air quality in megacities: A*  
686 *case study for Delhi*, *Atmospheric Environment*, 161, 99-111.
- 687 AQD, 2008. Directive 2008/50/EC of the European Parliament and of the Council of 21 May  
688 2008 on ambient air quality and cleaner air for Europe (No. 152). *Official Journal*.
- 689 Amato, F., Cassee, F.R., Denier van der Gon, H.A.C., Gehrig, R., Gustafsson, M., Hafner, W.,  
690 Harrison, R.M., Jozwicka, M., Kelly, F.J., Moreno, T., Prevot, A.S.H., Schaap, M.,  
691 Sunyer, J., Querol, X., 2014. *Urban air quality: The challenge of traffic non-exhaust*  
692 *emissions*. *Journal of Hazardous Materials* 275, 31–36.  
693 <https://doi.org/10.1016/j.jhazmat.2014.04.053>
- 694 ATMO2003: L'indice ATMO: indicateur de la qualité de l'air dans les agglomérations françaises  
695 [The ATMO index: an air quality indicator for developed areas in France]. *Eur Ann*  
696 *Allergy Clin Immunol.* 2003 May;35(5):166-9. French. PMID: 12838780.
- 697 ApSimon H., T. Oxley, H. Woodward, D. Mehlig, A. Dore, M. Holland, 2021. *The UK*  
698 *Integrated Assessment Model for source apportionment and air pollution policy*  
699 *applications to PM2.5*, *Environment International*, 153, 106515.
- 700 Belis, C.A., D. Pernigotti, G. Pirovano, O. Favez, J.L. Jaffrezo, J. Kuenen, H. Denier van Der  
701 Gon, M. Reizer, V. Riffault, L.Y. Alleman, M. Almeida, F. Amato, A. Angyal, G.  
702 Argyropoulos, S. Bande, I. Beslic, J.-L. Besombes, M.C. Bove, P. Brotto, G. Calori, D.  
703 Cesari, C. Colombi, D. Contini, G. De Gennaro, A. Di Gilio, E. Diapouli, I. El Haddad,  
704 H. Elbern, K. Eleftheriadis, J. Ferreira, M. Garcia Vivanco, S. Gilardoni, B. Golly, S.  
705 Hellebust, P.K. Hopke, Y. Izadmanesh, H. Jorquera, K. Krajsek, R. Kranenburg, P.  
706 Lazzeri, F. Lenartz, F. Lucarelli, K. Maciejewska, A. Manders, M. Manousakas, M.

707 Masiol, M. Mircea, D. Mooibroek, S. Nava, D. Oliveira, M. Paglione, M. Pandolfi, M.  
708 Perrone, E. Petralia, A. Pietrodangelo, S. Pillon, P. Pokorna, P. Prati, D. Salameh, C.  
709 Samara, L. Samek, D. Saraga, S. Sauvage, M. Schaap, F. Scotto, K. Segal, G. Siour, R.  
710 Tauler, G. Valli, R. Vecchi, E. Venturini, M. Vestenius, A. Waked, E. Yubero, 2020.  
711 Evaluation of receptor and chemical transport models for PM10 source apportionment,  
712 *Atmospheric Environment: X*, 5, 100053.

713 Bhavne P.V., Pouliot G.A. and Zheng M., 2007. Diagnostic model evaluation for carbonaceous  
714 PM2.5 using organic markers measured in the southeastern U.S. *Environmental Science  
715 and Technology* 41, 1577-1583.

716 Burr M.J. and Y. Zhang, 2011b. Source apportionment of fine particulate matter over the Eastern  
717 U.S. Part II: source sensitivity simulations using CAMX/PSAT and comparisons with  
718 CMAQ source sensitivity simulations, *Atmospheric Pollution Research*, 2, 318-336

719 Clappier A., E. Pisoni, P. Thunis, 2015. A new approach to design source-receptor relationships  
720 for air quality modelling. *Environmental Modelling & Software*, 74, 66-74.

721 Clappier A., C. Belis, D. Pernigotti and P. Thunis (2017) Source apportionment and sensitivity  
722 analysis: two methodologies with two different purposes. *Geosci. Model Dev. Discuss.*,  
723 <https://doi.org/10.5194/gmd-2017-161>, in review, 2017.

724 de Bruyn, S., de Vries, J., 2020. Health costs of air pollution in European cities and the linkage  
725 with transport (No. 20.190272.134). CE Delft, Delft.

726 Degraeuwe, B., Pisoni, E., Peduzzi, E., De Meij, A., Monforti-Ferrario, F., Bodis, K.,  
727 Mascherpa, A., Astorga-Llorens, M., Thunis, P. and Vignati, E., *Urban NO2 Atlas, EUR  
728 29943 EN*, Publications Office of the European Union, Luxembourg, 2019, ISBN 978-  
729 92-76-10386-8 (online), 978-92-76-10387-5 (print), doi:10.2760/43523  
730 (online), 10.2760/538816 (print), JRC118193.

731 De Meij, A., S. Wagner, N. Gobron, P. Thunis, C. Cuvelier, F. Dentener, M. Schaap, Model  
732 evaluation and scale issues in chemical and optical aerosol properties over the greater  
733 Milan area (Italy), for June 2001, *Atmos. Res.* 85, 243-267, 2007.

734 De Meij, A., Gzella, A., Cuvelier, C., Thunis, P., Bessagnet, B., Vinuesa, J.F., Menut, L., Kelder,  
735 H.M., 2009. The impact of MM5 and WRF meteorology over complex terrain on  
736 CHIMERE model calculations. *Atmospheric Chemistry and Physics* 9, 6611-6632.

737 De Meij, A., Bossioli, E., Vinuesa, J.F., Penard, C., Price, I., The effect of SRTM and Corine  
738 Land Cover on calculated gas and PM10 concentrations in WRF-Chem, *Atmos. Env.*  
739 Volume 101, Pages 177-193, January 2015.

740 De Meij, A., Zittis, G. & Christoudias, T., On the uncertainties introduced by land cover data in  
741 high-resolution regional simulations, *Meteorol. Atmos. Phys.* (2018).  
742 <https://doi.org/10.1007/s00703-018-0632-3>; <https://rdcu.be/38pt>

743 European Environment Agency. *Air Quality in Europe: 2020 Report*. Publications Office, 2020.  
744 DOI.org (CSL JSON), <https://data.europa.eu/doi/10.2800/786656>.

745 European Environment Agency, *Air quality in Europe — 2017 report*, No13/2017, ISSN 1977-  
746 8449, doi:10.2800/850018, [https://www.eea.europa.eu/publications/air-quality-in-europe-  
747 2017](https://www.eea.europa.eu/publications/air-quality-in-europe-2017).

748 European Commission. Joint Research Centre. Institute for Energy and Transport., 2014. Non-  
749 exhaust traffic related emissions - Brake and tyre wear PM: literature review.  
750 Publications Office, LU.

751 Grewe, V., E. Tsati, P. Hoor, 2010. On the attribution of contributions of atmospheric trace gases  
752 to emissions in atmospheric model applications, *Geosci. Model Dev.*, 3, 487-499

753 Grewe, V., K. Dahlmann, S. Matthes, W. Steinbrecht, 2012. Attributing ozone to NO<sub>x</sub>  
754 emissions: Implications for climate mitigation measures, *Atmos. Environ.*, 59, 102-107

755 Guo H., S. H. Kota, S. K. Sahu, J. Hu, Q. Ying, A. Gao, H. Zhang, 2017. Source apportionment  
756 of PM<sub>2.5</sub> in North India using source-oriented air quality models. *Environmental*  
757 *Pollution* 231, 426-436.

758 Hendriks C., R. Kranenburg, J. Kuenen, R. van Gijlswijk, R. Wichink Kruit, A. Segers, H.  
759 Denier van der Gon, M. Schaap, 2013. The origin of ambient particulate matter  
760 concentrations in the Netherlands, *Geosci. Model Dev.*, 6, 721–733, 2013

761 Huang Y., T. Deng, Z. Li, N. Wang, C. Yin, S. Wang, S. Fan, 2018. Numerical simulations for  
762 the sources apportionment and control strategies of PM<sub>2.5</sub> over Pearl River Delta, China,  
763 part I: Inventory and PM<sub>2.5</sub> sources apportionment, *Science of the Total Environment*  
764 634 (2018) 1631–1644.

765 Huszar, P., Belda, M., and Halenka, T.: On the long-term impact of emissions from central  
766 European cities on regional air quality, *Atmos. Chem. Phys.*, 16, 1331–1352,  
767 <https://doi.org/10.5194/acp-16-1331-2016>, 2016

768 Huszar, P., Karlický, J., Marková, J., Nováková, T., Liaskoni, M., and Bartík, L.: The regional  
769 impact of urban emissions on air quality in Europe: the role of the urban canopy effects,  
770 *Atmos. Chem. Phys.* [preprint], <https://doi.org/10.5194/acp-2021-355>, accepted for final  
771 publication, 2021.

772 Itahashi S., H. Hayami, K. Yumimoto, I. Uno, 2017. Chinese province-scale source  
773 apportionments for sulfate aerosol in 2005 evaluated by the tagged tracer method,  
774 *Environmental Pollution* 220, 1366-1375.

775 Jiang, L., Bessagnet, B., Meleux, F., Tognet, F., Couvidat, F., 2020. Impact of physics  
776 parameterizations on high-resolution air quality simulations over the Paris region.  
777 *Atmosphere* 11.

778 Kaspar R. Daellenbach, Gaëlle Uzu, Jianhui Jiang, Laure-Estelle Cassagnes, Zaira Leni,  
779 Athanasia Vlachou, Giulia Stafenelli, Francesco Canonaco, Samuël Weber, Arjo Segers,  
780 Jeroen J. P. Kuenen, Martijn Schaap, Olivier Favez, Alexandre Albinet, Sebnem  
781 Aksoyoglu, Josef Dommen, Urs Baltensperger, Marianne Geiser, Imad El Haddad, Jean-  
782 Luc Jaffrezo, André S. H. Prévôt. Sources of particulate-matter air pollution and its  
783 oxidative potential in Europe. *Nature*, 2020; 587 (7834): 414 DOI: 10.1038/s41586-020-  
784 2902-8

785 Keuken M., M. Moerman, M. Voogt, M. Blom, E.P. Weijers, T. Röckmann, U. Dusek (2013)  
786 Source contributions to PM<sub>2.5</sub> and PM<sub>10</sub> at an urban background and a street location,  
787 *Atmos. Environ.*, 71, 26–35.

788 Khomenko, S., Cirach, M., Pereira-Barboza, E., Mueller, N., Barrera-Gómez, J., Rojas-Rueda,  
789 D., de Hoogh, K., Hoek, G., Nieuwenhuijsen, M., 2021. Premature mortality due to air  
790 pollution in European cities: a health impact assessment. *The Lancet Planetary Health*  
791 S2542519620302722. [https://doi.org/10.1016/S2542-5196\(20\)30272-2](https://doi.org/10.1016/S2542-5196(20)30272-2)

792 Kieseewetter G. and Amann (2014). Urban PM<sub>2.5</sub> levels under the EU Clean Air Policy Package,  
793 IIASA TSAP Report 12.

794 Kieseewetter G., J. Borcken-Kleefeld, W. Schöpp, C. Heyes, P. Thunis, B. Bessagnet, E.  
795 Terrenoire, H. Fagerli, A. Nyiri and M. Amann (2015) Modelling street level PM<sub>10</sub>  
796 concentrations across Europe: source apportionment and possible futures, *Atmos. Chem.*  
797 *Phys.*, 15, 1539-1553.

798 Kranenburg R., Segers A., Hendriks C., and Schaap,. 2013. Source apportionment using  
799 LOTOS-EUROS: module description and evaluation, *Geosci. Model Dev.*, 6, 721–733

800 Kole, P.J., Löhr, A.J., Van Belleghem, F., Ragas, A., 2017. Wear and Tear of Tyres: A Stealthy  
801 Source of Microplastics in the Environment. *IJERPH* 14, 1265.  
802 <https://doi.org/10.3390/ijerph14101265>

803 Kwok R.H.F., S.L. Napelenok, K.R. Baker, 2013: Implementation and evaluation of PM2.5  
804 source contribution analysis in a photochemical model, *Atmospheric Environment* 80,  
805 398-407

806 Lavalle, C., Pontarollo, N., Batista E Silva, F., Baranzelli, C., Jacobs, C., Kavalov, B., Kompil,  
807 M., Perpiña Castillo, C., Vizcaino, M., Ribeiro Barranco, R., Vandecasteele, I., Pinto  
808 Nunes Nogueira Diogo, V., Aurambout, J., Serpieri, C., Marín Herrera, M., Rosina, K.,  
809 Ronchi, S. and Auteri, D., *European Territorial Trends - Facts and Prospects for Cities  
810 and Regions* Ed. 2017, EUR 28771 EN, Publications Office of the European Union,  
811 Luxembourg, 2017, ISBN 978-92-79-79906-8, doi:10.2760/28183, JRC107391.

812 Lenschow P., H.-J. Abraham, K. Kutzner, M. Lutz, J.-D. Preu, W. Reichenbacher (2001) Some  
813 ideas about the sources of PM10, *Atmospheric Environment* 35 Supplement No. 1 23–33.

814 Li Y., D. K. Henze, D. Jack, B. H. Henderson, P. L. Kinney, 2016. Assessing public health  
815 burden associated with exposure to ambient black carbon in the United States, *Science of  
816 the Total Environment* 539, 515–525.

817 Fei Liu, Z. Klimont, Qiang Zhang, J. Cofala, Lijian Zhao, Hong Huo, B. Nguyen, W. Schöpp, R.  
818 Sander, Bo Zheng, Chaopeng Hong, Kebin He, M. Amann, Ch. Heyes, 2013. Integrating  
819 mitigation of air pollutants and greenhouse gases in Chinese cities: development of  
820 GAINS-City model for Beijing, *Journal of Cleaner Production*, Volume 58, 25-33,  
821 <https://doi.org/10.1016/j.jclepro.2013.03.024>.

822 Luo H., L. Yang, Z. Yuan, K. Zhao, S. Zhang, Y. Duan, R. Huang, Q. Fu, 2020. Synoptic  
823 condition-driven summertime ozone formation regime in Shanghai and the implication  
824 for dynamic ozone control strategies, *Science of The Total Environment*, 745, 141130.

825 Mertens, M., Volker G., V.S. Rieger and P. Jöckel. Revisiting the contribution of land transport  
826 and shipping emissions to tropospheric ozone, *Atmos. Chem. Phys.*, 18, 5567–5588, 2018

827 Ntziachristos, L., Boulter, P., 2019. EMEP/EEA air pollutant emission inventory guidebook  
828 2019 - 1.A.3.b.vi Road transport: Automobile tyre and brake wear - 1.A.3.b.vii Road  
829 transport: Automobile road abrasion. European Environment Agency.

830 OECD (2012) *Redefining Urban: a new way to measure metropolitan areas*, OECD report,  
831 ISBN: 9789264174054, 148pp.

832 O'Neill, B. C., Dalton, M., Fuchs, R., Jiang, L., Pachauri, S., Zigova, K., *Global demographic  
833 trends and future carbon emissions*, *Proceedings of the National Academy of Sciences*  
834 Oct 2010, 107 (41) 17521-17526; DOI: 10.1073/pnas.1004581107.

835 Ortiz S. and Friedrich, R.: A modelling approach for estimating background pollutant  
836 concentrations in urban areas, *Atmos. Pollut. Res.*, 4, 147–156,  
837 doi:10.5094/APR.2013.015, 2013.

838 Osada, K., Ohara, T., Uno, I., Kido, M., Iida, H., 2009. Impact of Chinese anthropogenic  
839 emissions on submicrometer aerosol concentration at Mt. Tateyama, Japan. *Atmos.  
840 Chem. Phys.* 9 (23), 9111–9120.

841 Park, M., Joo, H.S., Lee, K. et al. Differential toxicities of fine particulate matters from various  
842 sources. *Sci Rep* 8, 17007 (2018). <https://doi.org/10.1038/s41598-018-35398-0>

843 Petetin H. M. Beekmann, J. Sciare, M. Bressi, A. Rosso, O. Sanchez and V. Ghers. (2014) A  
844 novel model evaluation approach focusing on local and advected contributions to urban  
845 PM2.5 levels – application to Paris, France, *Geosci. Model Dev.*, 7, 1483–1505.

846 Pey J., X. Querol and A. Alastuey, 2010, Discriminating the regional and urban contributions in  
847 the North-Western Mediterranean: PM levels and composition, *Atmospheric*  
848 *Environment* 44, 1587-1596.

849 Pisoni E., A. Clappier, B. Degraeuwe, P. Thunis, 2017. Adding spatial flexibility to source-  
850 receptor relationships for air quality modelling, *Environmental Modelling & Software*,  
851 90, 68-77.

852 Pisoni et al. 2021. A new methodology to evaluate the effectiveness of local policies during high  
853 PM2.5 episodes: application on 10 European cities. Submitted to *ACP*

854 Pommier, M., Fagerli, H., Schulz, M., Valdebenito, A., Kranenburg, R., and Schaap, M.:  
855 Prediction of source contributions to urban background PM10 concentrations in European  
856 cities: a case study for an episode in December 2016 using EMEP/MSC-W rv4.15 and  
857 LOTOS-EUROS v2.0 – Part 1: The country contributions, *Geosci. Model Dev.*, 13,  
858 1787–1807, <https://doi.org/10.5194/gmd-13-1787-2020>, 2020.

859 Qiao X., Q. Ying, X. Li, H. Zhang, J. Hu, Y. Tang, X. Chen, 2018. Source apportionment of  
860 PM2.5 for 25 Chinese provincial capitals and municipalities using a source-oriented  
861 Community Multiscale Air Quality model, *Science of the Total Environment* 612, 462–  
862 471.

863 Raifman, M., Russell, A. G., Skipper, T. N., & Kinney, P. L. (2020). Quantifying the health  
864 impacts of eliminating air pollution emissions in the city of boston. *Environmental*  
865 *Research Letters*, 15(9) doi:10.1088/1748-9326/ab842b

866 Schaap, M., Timmermans, R.M.A., Roemer, M., Boersen, G.A.C., Builtjes, P.J.H. Sauter, F.J.,  
867 Velders, G.J.M. and Beck, J.P. (2008) ‘The LOTOS–EUROS model: description,  
868 validation and latest developments’, *Int. J. Environment and Pollution*, Vol. 32, No. 2,  
869 pp.270–290.

870 Simpson, D., Benedictow, A., Berge, H., Bergström, R., Emberson, L. D., Fagerli, H., Flechard,  
871 C. R., Hayman, G. D., Gauss, M., Jonson, J. E., Jenkin, M. E., Nyíri, A., Richter, C.,  
872 Semeena, V. S., Tsyro, S., Tuovinen, J.-P., Valdebenito, Á., and Wind, P.: The EMEP  
873 MSC-W chemical transport model – technical description, *Atmos. Chem. Phys.*, 12,  
874 7825–7865, <https://doi.org/10.5194/acp-12-7825-2012>, 2012.

875 Squizzato S. and M. Masiol (2015) Application of meteorology-based methods to determine  
876 local and external contributions to particulate matter pollution: A case study in Venice  
877 (Italy), *Atmospheric Environment* 119, 69-81.

878 Timmermans R.M.A., H.A.C. Denier van der Gon, J.J.P. Kuenen, A.J. Segers, C. Honoré, O.  
879 Perrussel, P.J.H. Builtjes and M. Schaap (2013) Quantification of the urban air pollution  
880 increment and its dependency on the use of down-scaled and bottom-up city emission  
881 inventories, *Urban Climate* 6, 44–62.

882 UN, 2020 Policy Brief, Covid-19 in an urban world.  
883 [https://www.un.org/sites/un2.un.org/files/sg\\_policy\\_brief\\_covid\\_urban\\_world\\_july\\_2020](https://www.un.org/sites/un2.un.org/files/sg_policy_brief_covid_urban_world_july_2020.pdf)  
884 [.pdf](https://www.un.org/sites/un2.un.org/files/sg_policy_brief_covid_urban_world_july_2020.pdf)

885 Thunis, P., Degraeuwe, B., Peduzzi, E., Pisoni, E., Trombetti, M., Vignati, E., Wilson, J., Belis,  
886 C. and Pernigotti, D., *Urban PM2.5 Atlas: Air Quality in European cities*, EUR 28804  
887 EN, Publications Office of the European Union, Luxembourg, 2017, ISBN 978-92-79-  
888 73876-0 (online),978-92-79-73875-3 (print),978-92-79-75274-2 (ePub),

889 doi:10.2760/336669 (online),10.2760/851626 (print),10.2760/865663 (ePub),  
890 JRC108595.

891 Thunis P. (2018). On the validity of the incremental approach to estimate the impact of cities on  
892 air quality, *Atmospheric Environment*, 173, 210-222.

893 Thunis P., B. Degraeuwe, E. Pisoni, M. Trombetti, E. Peduzzi, C.A. Belis, J. Wilson, A.  
894 Clappier, E. Vignati, 2018. PM<sub>2.5</sub> source allocation in European cities: A SHERPA  
895 modelling study, *Atmospheric Environment*, 187, 93-106.

896 Tobías, A., Carnerero, C., Reche, C., Massagué, J., Via, M., Minguillón, M. C., . . . Querol, X.  
897 202). Changes in air quality during the lockdown in barcelona (spain) one month into the  
898 SARS-CoV-2 epidemic. *Science of the Total Environment*, 726  
899 doi:10.1016/j.scitotenv.2020.138540

900 Transboundary particulate matter, photo-oxidants, acidification and eutrophication components.  
901 Joint MSC-W & CCC & CEIP Report. EMEP Status Report 1/2017

902 United Nations, Department of Economic and Social Affairs, Population Division (2018), *The*  
903 *World's Cities in 2018 – Data Booklet (ST/ESA/SER.A/417)*.

904 Van Dingenen R., F. Dentener, M. Crippa, J. Leitaó, E. Marmer, S. Rao, E. Solazzo and L.  
905 Valentini, 2018. TM5-FASST: a global atmospheric source-receptor model for rapid  
906 impact analysis of emission changes on air quality and short-lived climate pollutants.  
907 *Atmospheric Chemistry and Physics*, <https://doi.org/10.5194/acp-2018-112>

908 Viana, M., Querol, X., Alastuey, A., Ballester, F., Llop, S., Esplugues, A., . . . Herce, M. D.  
909 (2008). Characterising exposure to PM aerosols for an epidemiological study.  
910 *Atmospheric Environment*, 42(7), 1552-1568. doi:10.1016/j.atmosenv.2007.10.087

911 Wagstrom, K. M., Pandis, S. N., Yarwood, G., Wilson, G. M., and Morris, R. E., 2008:  
912 Development and application of a computationally efficient particulate matter  
913 apportionment algorithm in a three dimensional chemical transport model, *Atmos.*  
914 *Environ.*, 42, 5650–5659.

915 Wang Z. S., Chien C.-J., and Tonnesen G. S., 2009. Development of a tagged species source  
916 apportionment algorithm to characterize three-dimensional transport and transformation  
917 of precursors and secondary pollutants, *J. Geophys. Res.*, 114, D21206

918 Wang L., Z. Wei, W. Wei, J. S. Fu, C. Meng, S. Ma, 2015. Source apportionment of PM<sub>2.5</sub> in  
919 top polluted cities in Hebei, China using the CMAQ model, *Atmospheric Environment*  
920 122, 723-736

921 Wang, L.T., Wei, Z., Yang, J., Zhang, Y., Zhang, F.F., Su, J., Meng, C.C., Zhang, Q., 2014. The  
922 2013 severe haze over southern Hebei, China: model evaluation, source apportionment,  
923 and policy implications. *Atmos. Chem. Phys.* 14, 3151-3173.

924 WHO2005, *Air Quality Guidelines Global Update 2005. Particulate matter, ozone, nitrogen*  
925 *dioxide and sulfur dioxide*, ISBN 92 890 2192 6

926 Wu, Q.Z., Wang, Z.F., Gbaguidi, A., Gao, C., Li, L.N., Wang, W., 2011. A numerical study of  
927 contributions to air pollution in Beijing during CAREBeijing-2006. *Atmos. Chem. Phys.*  
928 11 (12), 5997–6011.

929 Yarwood G., Morris R.E., and Wilson G.M, 2004. Particulate Matter Source Apportionment  
930 Technology (PSAT) in the CAMx Photochemical Grid Model. *Proceedings of the 27th*  
931 *NATO/ CCMS International Technical Meeting on Air Pollution Modeling and*  
932 *Application*. Springer Verlag  
933

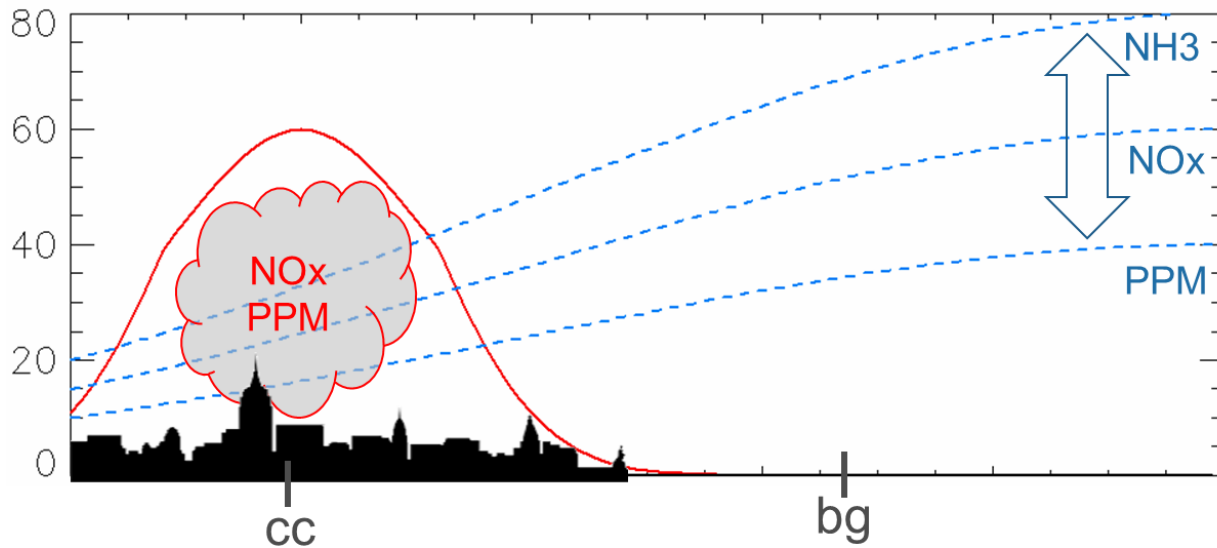


934 **Appendix A**

935 To illustrate the differences among SA methods, we use here the theoretical example  
 936 schematically represented in Figure A1. A city source (in red) emits with a Gaussian dispersion  
 937 profile both primary PM (PPM) and a gas-phase precursor (NO<sub>x</sub>). The background pollution (in  
 938 blue) is composed of a mix of NO<sub>x</sub>, NH<sub>3</sub> and PPM compounds. The various chemical reactions  
 939 that take place are simplified here for convenience into a single reaction. One mole of NH<sub>3</sub> reacts  
 940 with one mole of NO<sub>x</sub> to create one mole of ammonium nitrate (NH<sub>4</sub><sup>+</sup>NO<sub>3</sub><sup>-</sup>), i.e. secondary PM.  
 941 (NO<sub>x</sub> + NH<sub>3</sub> + X →→ NH<sub>4</sub><sup>+</sup>NO<sub>3</sub><sup>-</sup>). We assume here that the external compounds involved in the  
 942 reaction (X) are abundant and do not have a limiting effect on the formation of PM. While the  
 943 city emissions (source) remain unchanged, we modify the relative importance of the three  
 944 background compounds so that the background becomes in turn PPM, NO<sub>x</sub> and NH<sub>3</sub> dominated.  
 945 The PM concentration at a given location “x” is given by:

$$PM(x) = PPM(x) + \min\{NO_x(x), NH_3(x)\}_{mole} \times NH_4^+NO_3^- \quad (4)$$

947



948 *Figure A1: Schematic representation of the theoretical example used to compare the three SA approaches. The city source (in*  
 949 *red) emits NO<sub>x</sub> and PPM. The background (in blue, including other cities as well as rural sources) is composed of NO<sub>x</sub>, PPM and*  
 950 *NH<sub>3</sub> in different relative proportions (indicated by the arrow). The “cc” and “bg” symbols represent the city centre receptor and*  
 951 *the background location used for the increment approach, respectively.*

953 Based on the formulations provided in Table 1 and equation (4), the expressions to calculate the  
 954 city and background components for the theoretical example presented above are detailed in  
 955 Table A1. While these formulations are relatively straightforward for potential impacts and  
 956 increments, it is more complex for the tagging method. The city tagging component is the sum of  
 957 all PM species that are directly related to the city emissions. This includes PPM and NO<sub>3</sub> that are  
 958 related to the PPM and NO<sub>x</sub> city emissions, respectively. For the background component, it  
 959 includes PPM, NO<sub>x</sub> and also NH<sub>4</sub> that is related to the NH<sub>3</sub> emissions. Tagging allows following  
 960 the NO<sub>x</sub> and NH<sub>3</sub> emitted compounds through their chemical processes and transformations until  
 961 they create NO<sub>3</sub> and NH<sub>4</sub>, respectively that can be attributed to their respective sources. As NO<sub>x</sub>  
 962 is emitted by both sources, the total NO<sub>3</sub> must be fractioned and attributed to each single source.

963 In our example, the NO<sub>3</sub> fraction attributed to the city depends on the ratio of the available NO<sub>x</sub>  
 964 precursor at the location of interest ( $\beta = \frac{NO_{x\text{city}}(cc)}{NO_{x}(cc)}$ ). A similar process is used to calculate the  
 965 background component.

966  
 967 This example is used to compare the increment (INC), tagging (TAG) and potential impact (PI)  
 968 SA approaches.

969

Potential Impact	
City	$PM_{city}^{PI\alpha}(cc) = \frac{PM(cc) - PM_{city}^{\alpha}(cc)}{\alpha}$
Background	$PM_{bg}^{PI\alpha}(cc) = \frac{PM(cc) - PM_{bg}^{\alpha}(cc)}{\alpha}$
Increment	
City	$PM_{city}^{INC}(cc) = PM(cc) - PM(bg)$
Background	$PM_{bg}^{INC}(cc) = PM(bg)$
Tagging	
City	$PM_{city}^{TAG}(cc) = \sum_E^{city} PM_E(cc) = PPM_{E(PPM)_{city}}(cc) + \beta NO_3^-_{E(NO_2)_{city}}(cc)$
Background	$PM_{bg}^{TAG}(cc) = \sum_E^{bg} PM_E(cc) = PPM_{E(PPM)_{bg}}(cc) + (1 - \beta) NO_3^-_{E(NO_2)_{bg}}(cc) + NH_4^+_{E(NH_3)_{bg}}(cc)$

970 Table A1: Formulations for the potential impacts, increments and tagging approach for the example presented in Figure A1. The  
 971 indicator for all methods and components is the total particulate matter mass (PM). The SA method is indicated as superscript  
 972 (PI $\alpha$ , INC or TAG) whereas the source (city or bg) is in subscript. The receptor is the city center (cc) while the rural location  
 973 selected for the increment approach is denoted by "bg". For the tagging, the source subscript is also expressed directly as  
 974 emissions (E) distinguishing each compound (within brackets).

975 Figure A2 shows the city and background contributions obtained with the three SA methods,  
 976 differentiating two options for the PI one: 100% (PI100) and 20% reduction of the sources  
 977 (PI20). The figure also distinguishes four situations characterized by different background  
 978 compositions.

979

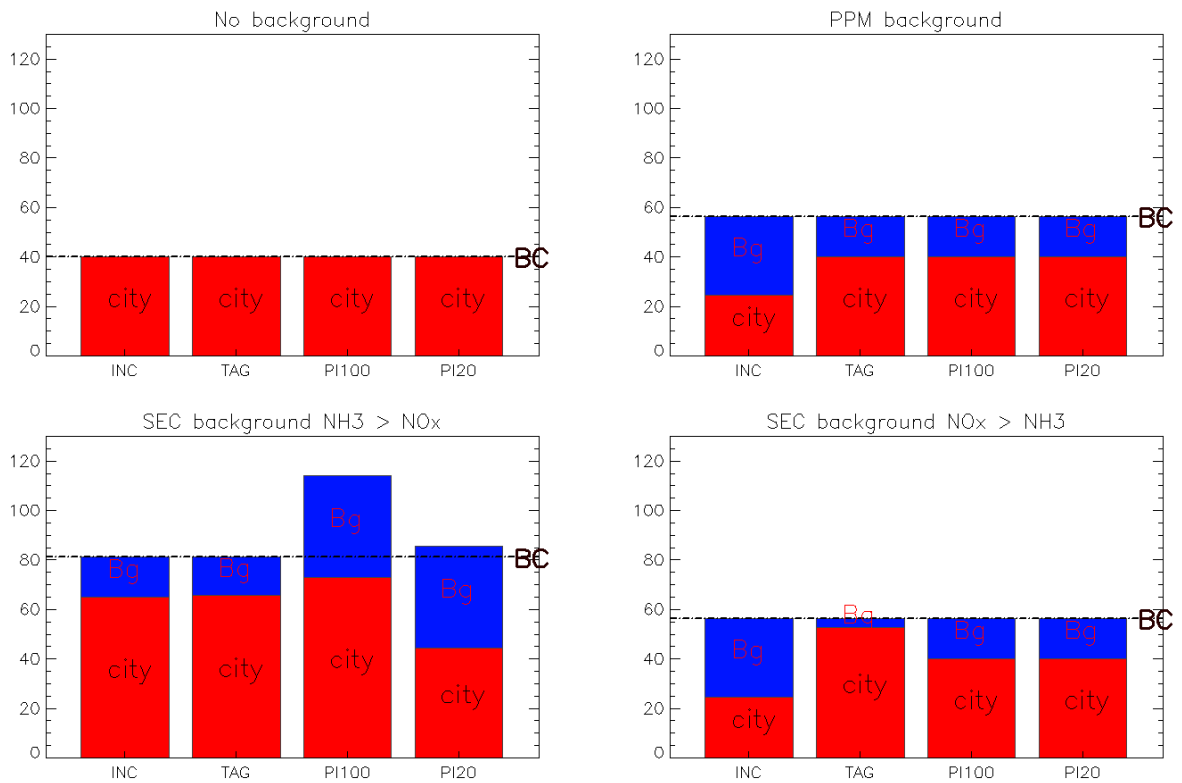
980 1. No background: When no background is present (top left), the city NO<sub>x</sub> emissions do not  
 981 form PM, only PPM emissions do. In such cases, all methods deliver the same response.

982

983 2. PPM background: When the background is composed of PPM only (top right), no  
 984 secondary species are formed. All methods agree with the exception of the increment  
 985 approach. This is due to the non-fulfilment of one of its underlying assumptions, i.e. the  
 986 lack of spatial homogeneity of the background which affects differently the rural and city  
 987 locations (indicated by "cc" and "bg" in Figure A2, respectively).

988

- 989 3. SEC background with  $\text{NH}_3 > \text{NO}_x$ : When secondary background precursors ( $\text{NO}_x$  and  
 990  $\text{NH}_3$ ) reach the city (bottom row), SA methods deliver different results because they  
 991 manage differently non-linear processes. When  $\text{NH}_3$  is more abundant than  $\text{NO}_x$  (bottom  
 992 left), the PI100 method does not preserve additivity (discussed in the “concepts” section),  
 993 i.e. the sum of the two components exceeds the total PM concentration. As seen from the  
 994 results and also from Table A1, this is not the case for the increment and tagging  
 995 approaches that are constructed to be additive.  
 996  
 997 4. SEC background with  $\text{NH}_3 < \text{NO}_x$ : When  $\text{NH}_3$  is less abundant than  $\text{NO}_x$  (bottom right),  
 998 differences remain important between the tagging, potential impacts and increment  
 999 approaches but additivity is preserved for both PI100 and PI10 that provide identical  
 1000 responses.



1001  
 1002 *Figure A2: Comparison of the city (red) and background (blue) components for 4 approaches applied on the theoretical examples*  
 1003 *described in Figure A1. Results are expressed for different types of background: (top left) no background; (top right) background*  
 1004 *limited to PPM; (bottom left) background limited to secondary but with  $\text{NH}_3 > \text{NO}_x$  and (bottom right) background limited to*  
 1005 *secondary but with  $\text{NH}_3 < \text{NO}_x$ .*